UCB-NE-5005

Effects of Far-Field Region as a Natural Barrier

—Analysis for KHNP LLW Repository—

D. Kawasaki, J. Ahn, P. L. Chambré
Department of Nuclear Engineering
Univerisity of California, Berkeley

June 18, 2004

The authors invite comments and would appreciate being notified of any errors in the report.

Joonhong Ahn
Department of Nuclear Engineering
University of California
Berkeley, CA 94720-1730
USA

ahn@nuc.berkeley.edu

Contents

1 Introduction

This report describes results of the collaborative project performed between Nuclear Environment Technology Institute, Korea Hydro & Nuclear Power Co. Ltd. (KHNP-NETEC hereafter) and the Department of Nuclear Engineering, University of California, Berkeley (UCB-NE hereafter).

UCB-NE developed the multi-compartment model and the computer code, Virtual Repository (VR), for radionuclide transport in the region interior to the repository [1, 2, 3, 4]. The repository region is divided into compartments, each containing a waste canister, the surrounding EBS, and the near-field rock region. There are the same number of compartments as that of the canisters placed in the repository. Radionuclide transport in compartments included in the same water stream is connected by advective transport assumed in the near-field region of each compartment. Canister-array configuration relative to water flow direction, multi-member decay chains, solubility sharing among isotopes of the same element, and release rate determined by congruency and solubility limit mechanism are also taken into account. The VR model is thus capable of reflecting the details of repository design, such as the size of the repository and arrangement of the waste canisters.

KHNP-NETEC is currently undertaking the performance assessment study for a low-level waste (LLW) repository with its Safety Assessment Groundwater Evaluation (SAGE) code [5, 6, 7]. A site for the LLW disposal has not yet been determined in Korea. The code, developed primarily for a generic assessment, includes conceptual models for radionuclide release from degrading engineered barriers to an underlying unsaturated zone, and to a water-saturated zone. The code also has flexibility to analyze site-specific, design-specific assessments with necessary modifications. In SAGE, the near field consists of a series of compartments that represent the waste form, the EBS and the unsaturated zone.

Presently, at KHNP-NETEC, a design of a LLW repository is being developed. Among many engineering challenges, it is of particular importance to find an optimum arrangement of vaults in the repository area to minimize the radionuclide flux and concentration at the interface between the geosphere and biosphere (GBI), and to minimize the environmental impact of the repository. It is considered that we need a model of radionuclide transport both in the near and far fields that incorporates the arrangement of vaults properly and calculates the fluxes, concentrations, and mass distributions of radionuclides as functions of time. The multi-compartment model and its numerical code, VR-KHNP, has been developed for this purpose. The VR-KHNP code has been successfully developed with the OCTAVE environment, which is similar to MATLAB.

The VR-KHNP model inherits the features of basic governing equations from the original VR model, and the geometric configuration of the repository site from SAGE. The waste vault, unsaturated soil, and aquifer regions in near and far fields are divided into compartments. The VR-KHNP code calculates mass, flux, and concetration of a radionuclide in each compartment as functions of time. It takes into account

multi-member decay chain, and arrangement and dimensions of the waste form, the engineered barrier system (EBS), and the geological media. In the VR-KHNP model, all the physical and hydraulic properties in a compartment are integrated into the average residence time of a nuclide in the compartment. In this report, we attempt to explain behavior of a radionuclide in terms of the residence times and its half-life.

In the previous studies with VR [1, 2], effects of the canister-array configuration on the radionuclide release rate at the near-field/far-field interface (NFI) were investigated. The present model for VR-KHNP is also capable of observing the effects of detailed configuration in the repository since shape, size, and heterogeneity of the repository are taken into account. In addition, radionuclide transport through the aquifer at far field is also modeled together with transport at near field in VR-KHNP. Because radionuclides attenuate by radioactive decay and are dispersed through migration in the far-field aquifer region, the far-field aquifer region can be considered as a natural barrier between repository and the environment. Effects of the far-field aquifer transport are investigated for various nuclides in this report.

With the VR-KHNP code, preliminary investigation is made for effects of vault-array configuration in conjunction with the water flow direction. It is observed that for some radionuclides such as ^{63}Ni, ^{99}Tc, and ^{137}Cs repository configuration has significant effects on their release rate at the NFI. Also observed is the environmental impact of the repository, in terms of the radio-toxicity of radionuclides that exist in the biosphere.

2 Physical Processes

The low-level waste repository in consideration consists of the waste and concrete vault surrounding the waste placed in the unsaturated soil.

Radionuclide transport and release from a repository is initiated by water contact after the cover materials fail. In the subsurface environment, failure of the cover occurs gradually, which results in water percolating into the waste form at a rate gradually increasing with time. In the present model, this hydraulic evolution is described by applying a piecewise step function with time to the infiltration rate of water flowing through the repository region. Eventually, this infiltration rate reaches the ambient infiltration rate. It is assumed that the flow through the disposal facility is uniformly distributed and steady.

Once water enters the waste facility through the failed cover, radionuclides dissolve into the water, the waste form is degraded into a porous medium, and the water partially saturates the degraded waste form. Radionuclides residing in disposed materials that are simply dumped into the vault or mixed with concrete are expected to quickly dissolve into water upon water contact. It is conservatively assumed in the present study that dissolution of these radionuclides happens instantaneously. The concentrations of dissolved nuclides are expected to be lower than the their solubilities for the LLW repository. Limitation of radionuclide dissolution due to a low solubility is not considered.

Water flows in a vertical direction in unsaturated media. Radionuclides dissolved in the water are transported into the concrete region, into the unsaturated soil region, and then into the aquifer via advection. Effect of molecular diffusion is neglected. It is assumed that the degrading waste form is a porous material with pores partially filled with water, and that the moisture content is steady and uniform throughout the waste form. Sorption equilibrium with a linear isotherm between the solid phase and the water phase is assumed everywhere.

Groundwater flows in a horizontal direction at a constant and uniform velocity in the aquifer, and radionuclides that has entered the aquifer are transported horizontally by advection.

Radionuclide transport in a LLW repository and in the aquifer below it is modeled by considering a set of hypothetical compartments. Schematic diagram of repository structure is shown in Figure 5.1. Within a compartment, properties of the medium are considered to be uniform. It is assumed that radionuclides in a compartment are instantaneously mixed, and that concentration is spatially uniform within the compartment.

Three compartments in the unsaturated zone represents the waste, concrete, and soil compartments. These compartments have the same cross-sectional area A_m perpendicular to the groundwater flow. Aquifer is divided into a series of compartments of identical dimensions. The effect of mechanical dispersion in the longitudinal direction is mimicked by the series of multiple compartments. The dimension of an aquifer compartment in the flow direction is determined from the longitudinal dispersivity.

3 Mathematical Formulation

3.1 Unsaturated Zone

We assume that, at time $t = 0\,[\mathrm{yr}]$, all radionuclides contained in the waste matrix instantaneously dissolve in the groundwater in the waste compartment. We also assume that sorption equilibrium between solid phase and liquid phase is established all the time. As the groundwater flows through the waste compartment, the radionuclide dissolved in the water also moves and flows into the adjacent concrete compartment. The radionuclide mass in the waste compartment changes with time because of this release and radioactive decay. The radionuclide that has entered the other UZ compartments similarly migrates by advection while it also undergo radioactive decay.

Distribution of a radionuclide is described by the assumed uniform concentration $C_{l,m}^{(i)}\,[\mathrm{mol/m^3}]$ in the liquid phase of each compartment. The mass balance equations in the unsaturated compartments, including the waste, concrete, and unsaturated soil, are written as follows in terms of $C_{l,m}^{(i)}$:

$$R_{l,m}^{(i)} s_{l,m} \epsilon_{l,m} V_{l,m} \frac{\mathrm{d}C_{l,m}^{(i)}}{\mathrm{d}t} = A_l q_k C_{l,m-1}^{(i)}(t) - A_l q_k C_{l,m}^{(i)}(t) + \lambda^{(i-1)} R_{l,m}^{(i-1)} s_{l,m} \epsilon_{l,m} V_{l,m} C_{l,m}^{(i-1)}(t) - \lambda^{(i)} R_{l,m}^{(i)} s_{l,m} \epsilon_{l,m} V_{l,m} C_{l,m}^{(i)}(t)\,, \quad (3.1)$$

with

$$C_{l,m}^{(0)}(t) \equiv 0\,, \quad C_{l,0}^{(i)}(t) \equiv 0\,,$$

for

$$t_k < t < t_{k+1}\,, \quad i = 1, 2, \ldots, i_0\,, \quad k = 0, 1, \ldots, k_0\,, \quad l = 1, 2, \ldots, l_0\,, \quad m = 1, 2, 3\,.$$

Superscript i denotes that the symbol is for the ith nuclide of the radioactive decay chain. Subscript k is the index for time domain. Subscript l denotes that the symbol is for the waste zone l or for the UZ compartments below it. Multiple waste zones are applied in configuration models C and D mentioned later in Figure 5.1. Subscript m denotes the waste compartment ($m = 1$), the compartment for the concrete wall ($m = 2$), and the unsaturated soil compartment ($m = 3$).

The first and the second terms on the right side of Eq. (3.1) are the advective flow rate of the radionuclide i into and out from the compartment, respectively, where $A_l\,[\mathrm{m^2}]$ is the horizontal cross-sectional area of the compartments, and $q_k\,[\mathrm{m/yr}]$ is the Darcy velocity of groundwater in the unsaturated zone during the time domain $t_k < t < t_{k+1}$. The Darcy velocity in the UZ is assigned a different value for each time domain in order to describe the changing infiltration rate due to gradual degradation of the cover materials of the waste vault in the early times. We assume that Darcy velocity in the UZ is spatially uniform.

The third and the fourth terms on the right side are the gain and the loss of the radionuclide i due to radioactive decay of nuclide i and its parent nuclide $i-1$. The symbol $\lambda^{(i)}$ [yr^{-1}] denotes the radioactive decay constant of nuclide i; $s_{l,m}$, $\epsilon_{l,m}$ are the saturation and the porosity in the compartment, respectively. Volume of the compartment, $V_{l,m}$ [m^3], is described with the cross-sectional area A_l and the vertical dimension $L_{l,m}$ [m] of the compartment as

$$V_{l,m} = A_l L_{l,m} \,. \tag{3.2}$$

Sorption equilibrium with a linear isotherm between the solid phase and the water phase is assumed. The retardation factor $R^{(i)}_{l,m}$ is defined as

$$R^{(i)}_{l,m} \equiv 1 + \frac{(1-\epsilon_{l,m})\rho_{l,m} K^{(i)}_{\mathrm{d}l,m}}{s_{l,m}\epsilon_{l,m}} \,, \tag{3.3}$$

where $K^{(i)}_{\mathrm{d}l,m}$ [m^3/kg] is the sorption distribution coefficient of the ith nuclide in the compartment, $\rho_{l,m}$ [kg/m^3] is the material density of the solid.

The total mass $M^{(i)}_{l,m}$ [mol] of the ith radionuclide in a compartment is written as

$$M^{(i)}_{l,m}(t) \equiv R^{(i)}_{l,m} s_{l,m}\epsilon_{l,m} V_{l,m} C^{(i)}_{l,m}(t) \,. \tag{3.4}$$

The mass balance equation (3.1) can be rewritten with masses $M^{(i)}_{l,m}$ as follows:

$$\frac{\mathrm{d}M^{(i)}_{l,m}}{\mathrm{d}t} = \mu^{(i)}_{k,l,m-1} M^{(i)}_{l,m-1}(t) - \mu^{(i)}_{k,l,m} M^{(i)}_{l,m}(t) \lambda^{(i-1)} M^{(i-1)}_{l,m}(t) - \lambda^{(i)} M^{(i)}_{l,m}(t) \,, \tag{3.5}$$

with

$$M^{(0)}_{l,m}(t) \equiv 0 \,, \quad M^{(i)}_{l,0}(t) \equiv 0 \,,$$

for

$$t_k < t < t_{k+1} \,, \quad i = 1, 2, \ldots, i_0 \,, \quad k = 0, 1, \ldots, k_0 \,, \quad l = 1, 2, \ldots, l_0 \,, \quad m = 1, 2, 3 \,.$$

All terms in Eq. (3.5) correspond to the terms in Eq. (3.1) in the same order. Rate coefficient $\mu^{(i)}_{k,l,m}$ [yr^{-1}] is defined as

$$\mu^{(i)}_{k,l,m} \equiv \frac{A_l q_k}{R^{(i)}_{l,m} s_{l,m}\epsilon_{l,m} V_{l,m}} = \frac{v_{k,l,m}}{R^{(i)}_{l,m} L_{l,m}} \,, \tag{3.6}$$

where $v_{k,l,m}$ [m/yr] is the pore velocity of groundwater in the compartment. The second equality in Eq. (3.6) is obtained by substituting Eq. (3.2) and the following relationship:

$$q_k = s_{l,m}\epsilon_{l,m} v_{k,l,m} \,. \tag{3.7}$$

The reciprocal $1/\mu^{(i)}_{k,l,m}$ [yr] is interpreted as the average time it takes for the ith nuclide to migrate the compartment length $L_{m,l}$ by advection, or the *average residence time* of the nuclide in the compartment.

We assume that all radionuclides in the waste form dissolve in groundwater and reach the sorption equilibria instantaneouly in waste compartments at time $t = 0$. We also assume that no radionuclide initially exists in the concrete compartment or in the soil compartment. These are described by the following initial conditions for $M_{l,m}^{(i)}$:

$$M_{l,1}^{(i)}(0) = M_l^{0(i)}\,, \quad M_{l,2}^{(i)}(0) = M_{l,3}^{(i)}(0) = 0\,, \tag{3.8}$$

$$\text{for} \quad i = 1, 2, \ldots, i_0\,, \quad l = 1, 2, \ldots, l_0\,. \tag{3.9}$$

3.2 Saturated Zone

Radionuclides that have been released from the UZ soil compartment (which is located at the bottom of the unsaturated zone) enter the aquifer compartments directly below the UZ soil compartment. Groundwater flows in the horizontal direction in the aquifer, and the multiple compartments are arranged as an array in the flow direction. Radionuclides in the aquifer are transported from a compartment to another by advection.

As in the case for the UZ compartments, distribution of a nuclide in an aquifer compartment is represented by the concentration uniformized over the whole compartment. The mass balance equation of the ith nuclide in the nth compartment in the saturated zone is formulated as follows

$$\begin{aligned} R_{\mathrm{SZ}}^{(i)} s_{\mathrm{SZ}} \epsilon_{\mathrm{SZ}} V_{\mathrm{SZ}} \frac{\mathrm{d}C_{\mathrm{SZ}n}^{(i)}}{\mathrm{d}t} = & \sum_{l=1}^{l_0} a_{l,n} A_l q_k C_{l,3}^{(i)} + A_{\mathrm{SZ}} q_{\mathrm{SZ}} C_{\mathrm{SZ}n-1}^{(i)}(t) - A_{\mathrm{SZ}} q_{\mathrm{SZ}} C_{\mathrm{SZ}n}^{(i)}(t) \\ & + \lambda^{(i)} R_{\mathrm{SZ}}^{(i-1)} s_{\mathrm{SZ}} \epsilon_{\mathrm{SZ}} V_{\mathrm{SZ}} C_{\mathrm{SZ}n}^{(i-1)}(t) - \lambda^{(i)} R_{\mathrm{SZ}}^{(i)} s_{\mathrm{SZ}} \epsilon_{\mathrm{SZ}} V_{\mathrm{SZ}} C_{\mathrm{SZ}n}^{(i)}(t)\,, \end{aligned} \tag{3.10}$$

with

$$C_{\mathrm{SZ}0}^{(i)}(t) = 0\,, \quad C_{\mathrm{SZ}n}^{(0)}(t) = 0\,,$$

for

$$t_k < t < t_{k+1}\,, \quad i = 1, 2, \ldots, i_0\,, \quad k = 0, 1, \ldots, k_0\,, \quad n = 1, 2, \ldots, N\,.$$

Subscript SZ denotes that the symbol represents a property in the saturated zone (aquifer). Subscript n indicates the position of the compartment in the aquifer; $n = 1$ denotes the compartment at the upstream end of the array, and $n = N$ at the downstream end. The concentration of the ith radionuclide in the water phase in compartment n is denoted as $C_{\mathrm{SZ}n}^{(i)}$ [mol/m^3].

The first term in the right side of Eq. (3.10) is the sum of the flow rates of the ith nuclide that enters the nth aquifer compartment from the UZ soil compartments above it. In case a UZ soil compartment has direct contact with multiple aquifer compartments, the flow of grounwater from the UZ soil compartment into the aquifer is split into fractions and is distributed over the multipla aquifer compartments. The fraction of flow rate into the nth aquifer compartment is proportional to the interfacial area between the

nth aquifer compartment and the UZ soil compartment. Hence, $a_{l,n}A_l q_k$ represents the rate of water flowing into the nth compartment from the UZ soil compartment below the waste zone l, where $a_{l,n}$ is the ratio of the above-mentioned interfacial area to the cross-sectional area of the entire soil compartment, A_l.

The second and the third terms in the right side of Eq. (3.10) represent the advective flow rate of the ith nuclide into and out from the compartment n, where q_{SZ} [m/yr] is the Darcy velocity of water in the aquifer, and A_{SZ} [m^2] is the cross-sectional area of the aquifer compartments perpendicular to the flow direction. The Darcy velocity and pore velocity v_{SZ} in the aquifer are interexchangeable with the following relationship:

$$q_{\mathrm{SZ}} = s_{\mathrm{SZ}}\epsilon_{\mathrm{SZ}}v_{\mathrm{SZ}}\,, \tag{3.11}$$

where s_{SZ} and ϵ_{SZ} are saturation and porosity in the aquifer, respectively. The aquifer is assumed to be fully saturated with water ($s_{\mathrm{SZ}} = 1$). Unlike the Darcy velocity q_k in the UZ compartments, the Darcy velocity q_{SZ} in the aquifer is assumed to be commonly constant for all time domains.

The fourth and the fifth terms in Eq. (3.10) represent the mass gain of the ith nuclide by radioactive decay of the parent nuclide $i-1$ in the decay chain, and the loss by radioactive decay of the ith nuclide itself, respectively. The volums of an aquifer compartment, V_{SZ} [m^3], is determined by

$$V_{\mathrm{SZ}} \equiv A_{\mathrm{SZ}}L_{\mathrm{SZ}}\,, \tag{3.12}$$

where L_{SZ} [m] is the length of an aquifer compartment (which is in turn determined in Section 3.5). Sorption equilibrium is assumed, and the retardation factor $R^{(i)}_{\mathrm{SZ}}$ is defined as

$$R^{(i)}_{\mathrm{SZ}} \equiv 1 + \frac{(1-\epsilon_{\mathrm{SZ}})\rho_{\mathrm{SZ}}K^{(i)}_{\mathrm{dSZ}}}{s_{\mathrm{SZ}}\epsilon_{\mathrm{SZ}}}\,, \tag{3.13}$$

where ρ_{SZ} [kg/m^3] is the material density of the solid phase in the aquifer, and $K^{(i)}_{\mathrm{dSZ}}$ [m^3/kg] is the sorption distribution coefficient of the ith nuclide in the aquifer.

The mass of the ith radionuclide in the nth aquifer compartment is written as

$$M^{(i)}_{\mathrm{SZ}n}(t) \equiv R^{(i)}_{\mathrm{SZ}}s_{\mathrm{SZ}}\epsilon_{\mathrm{SZ}}V_{\mathrm{SZ}}C^{(i)}_{\mathrm{SZ}n}(t)\,. \tag{3.14}$$

Substituting this into Eq. (3.10), the mass balance equation in the nth aquifer compartment is rewritten in terms of $M^{(i)}_{\mathrm{SZ}n}$ as follows:

$$\frac{\mathrm{d}M^{(i)}_{\mathrm{SZ}n}}{\mathrm{d}t} = \sum_{l=1}^{l_0} a_{l,n}\mu^{(i)}_{k,l,3}M^{(i)}_{l,3}(t) + \mu^{(i)}_{\mathrm{SZ}}M^{(i)}_{\mathrm{SZ}n-1}(t) - \mu^{(i)}_{\mathrm{SZ}}M^{(i)}_{\mathrm{SZ}n}(t) + \lambda^{(i-1)}M^{(i-1)}_{\mathrm{SZ}n}(t) - \lambda^{(i)}M^{(i)}_{\mathrm{SZ}n}(t)\,, \tag{3.15}$$

with

$$M^{(i)}_{\mathrm{SZ}0}(t) = 0\,, \quad M^{(0)}_{\mathrm{SZ}n}(t) = 0\,,$$

for

$$t_k < t < t_{k+1}\,, \quad i = 1, 2, \ldots, i_0\,, \quad k = 0, 1, \ldots, k_0\,, \quad n = 1, 2, \ldots, N\,.$$

All terms in Eq. (3.15) correspond to the terms in Eq. (3.10) in the same order. Rate coefficient $\mu_{\mathrm{SZ}}^{(i)}\,[\mathrm{yr}^{-1}]$ is defined as

$$\mu_{\mathrm{SZ}}^{(i)} \equiv \frac{A_{\mathrm{SZ}} q_{\mathrm{SZ}}}{R_{\mathrm{SZ}}^{(i)} s_{\mathrm{SZ}} \epsilon_{\mathrm{SZ}} V_{\mathrm{SZ}}} = \frac{v_{\mathrm{SZ}}}{R_{\mathrm{SZ}}^{(i)} L_{\mathrm{SZ}}}\,, \tag{3.16}$$

where the second equality is obtained by substituting Eqs. (3.11) and (3.12). $1/\mu_{\mathrm{SZ}}^{(i)}\,[\mathrm{yr}]$ is interpreted as the average time it takes for the ith nuclide to migrate the length of a single aquifer compartment, L_{SZ}, or the average residence time of the nuclide in a compartment.

It is assumed that there is initially no radionuclide in the aquifer. Therefore the governing equations (3.15) are subject the following initial conditions:

$$M_{\mathrm{SZ}n}^{(i)}(0) = 0\,, \quad i = 1, 2, \ldots, i_0\,, \quad n = 1, 2, \ldots, N\,. \tag{3.17}$$

3.3 Release Rate

The release rate of the ith radionuclide from a compartment is given by

$$J_{l,m}^{(i)}(t) \equiv A_l q_k C_{l,m}^{(i)}(t) = \mu_{k,l,m}^{(i)} M_{l,m}^{(i)}(t)\,, \tag{3.18}$$
$$\text{for} \quad t_k < t < t_{k+1}\,, \quad i = 1, 2, \ldots, i_0\,, \quad k = 0, 1, \ldots, k_0\,, \quad l = 1, 2, \ldots, l_0\,, \quad m = 1, 2, 3\,,$$

in the UZ compartments, and

$$J_{\mathrm{SZ}n}^{(i)}(t) \equiv A_{\mathrm{SZ}} q_{\mathrm{SZ}} C_{\mathrm{SZ}n}^{(i)}(t) = \mu_{\mathrm{SZ}}^{(i)} M_{\mathrm{SZ}n}^{(i)}(t)\,, \tag{3.19}$$
$$i = 1, 2, \ldots, i_0\,, \quad n = 1, 2, \ldots, N\,,$$

in the aquifer compartments. This release rate is provided as one the direct output data from the VR-KHNP calculation.

We define the fractional release rate $f_n^{(i)}\,[\mathrm{yr}^{-1}]$ from the nth aquifer compartment for nuclide i as

$$f_n^{(i)}(t) \equiv \frac{\mu_{\mathrm{SZ}}^{(i)} M_{\mathrm{SZ}n}^{(i)}(t)}{\sum_l M_l^{0(i)}}\,, \quad t > 0 \tag{3.20}$$

where $\sum_l M_l^{0(i)}$ is the initial inventory of the radionuclide i in the entire repository. Similarly, we define the fractional release rate $f_n^{\mathrm{chain}}\,[\mathrm{yr}^{-1}]$ for an entire decay chain as

$$f_n^{\mathrm{chain}}(t) \equiv \frac{\sum_i \mu_{\mathrm{SZ}}^{(i)} M_{\mathrm{SZ}n}^{(i)}(t)}{\sum_i \sum_l M_l^{0(i)}}\,, \quad t > 0\,, \tag{3.21}$$

where the numerator of the right side is the sum of release rates of all the member nuclides in the decay chain, and the denominator is the sum of initial inventories of whole decay chain members in the entire repository.

3.4 Mass in the Environment

The radionuclides released from the last aquifer compartment through the GBI enter the environment. The mass of the radionuclide in the environment is controled by the flux at the GBI and the radioactive decay:

$$\frac{\mathrm{d}M_{\mathrm{env}}^{(i)}}{\mathrm{d}t} = \lambda^{(i-1)} M_{\mathrm{env}}^{(i-1)}(t) + \mu_{\mathrm{SZ}}^{(i)} M_{\mathrm{SZ}N}^{(i)}(t) - \lambda^{(i)} M_{\mathrm{env}}^{(i)}(t)\,. \tag{3.22}$$

It is assumed that there is initially no radionuclide in the environment.

$$M_{\mathrm{env}}^{(i)}(0) = 0\,. \tag{3.23}$$

In order to discuss the consequences of the repository impact to the environment, we consider the environmental impact. The environmental impact is defined as radiotoxicity index of the radionuclides that exist in the environment [8]. The radiotoxicity of a radionuclide is obtained by dividing the radioactivity by the maximum permissible concentration for ingestion [9]. The toxicity index of the radionuclide in the environment is obtained as

$$\text{toxicity}\,[\mathrm{m}^3] = \frac{\lambda^{(i)} M_{\mathrm{env}}^{(i)}(t)}{C_{\mathrm{MPC}}^{(i)}}\,, \tag{3.24}$$

where $C_{\mathrm{MPC}}^{(i)}\,[\mathrm{Ci/m}^3]$ is the maximum permissible concentration of the radionuclide in water set by a regulation. The radiotoxicity index has the unit of water volume, with which the radionuclide is diluted to the concentration of a tolerable level.

3.5 Size of Compartments in the Saturated Zone

To describe the relationship between the length of a SZ compartment, L_{SZ}, and the longitudinal dispersivity α, we will discuss on a special problem only for this purpose.

We consider a series of SZ compartments ($n = 1, \ldots, N$) but no UZ compartments on top of it. We assume that, at time $t = 0$, a unit mass of a stable nuclide is injected to the first SZ compartment at once. All the other compartments do not contain the nuclide initially. The governing equations are written as

$$\frac{\mathrm{d}M_n}{\mathrm{d}t} = \mu M_{n-1}(t) - \mu M_n(t)\,, \quad t > 0\,, \quad n = 1, 2, \ldots, N\,, \tag{3.25}$$

subject to

$$M_n(0) = 1\,, \quad \text{and} \quad M_0(t) = 0\,, \quad t \geq 0\,,$$

where M_n is the mass of the nuclide in the nth compartment, μ corresponds to $\mu_{\mathrm{SZ}}^{(i)}$ and is defined as $\mu \equiv v/RL$ (see Eq. (3.16)).

As the solution to the above equations, the mass of the nuclide in the nth compartment at time t (≥ 0) is expressed as

$$M_n(t) = \frac{(\mu t)^{n-1}}{(n-1)!} e^{-\mu t} . \tag{3.26}$$

This is mathematically in the same form as the probability mass function, f_{p}, of Poisson distribution with mean $m_{\mathrm{p}} = \mu t$:

$$f_{\mathrm{p}}(n') = \frac{m_{\mathrm{p}}^{n'}}{n'!} e^{-m_{\mathrm{p}}} , \tag{3.27}$$

where n' in Eq. (3.27) corresponds to $n-1$ in Eq. (3.26). This distribution has the standard deviation

$$\sigma_{\mathrm{p}} = \sqrt{m_{\mathrm{p}}} = \sqrt{\mu t} .$$

This standard deviation represents *the extent of the nuclide dispersion* at time t, in terms of the number of compartments. The extent of the nuclide dispersion can be expressed in terms of distance as $\sigma_{\mathrm{p}} L$, where L is the length of a compartment.

Now, we consider the dispersion problem in one dimensional infinite medium:

$$R\frac{\partial C}{\partial t} = D\frac{\partial^2 C}{\partial x^2} - Rv\frac{\partial C}{\partial x} .$$

We consider a situation similar to the compartment counterpart. We assume a pulsewise injection of a unit mass of the stable nuclide at $x = 0$, $t = 0$. The solution is written as

$$C(x,t) = \frac{1}{2\sqrt{\pi\, Dt/R}} \exp\left(-\frac{(x - vt/R)^2}{4Dt/R}\right) . \tag{3.28}$$

This is mathematically in the same form as the probability density function, f_{n}, of the normal distribution with mean $m_{\mathrm{n}} = vt/R$ and standard deviation $\sigma_{\mathrm{n}} = \sqrt{2Dt/R}$:

$$f_{\mathrm{n}}(x) = \frac{1}{\sqrt{2\pi}\,\sigma_{\mathrm{n}}} \exp\left(-\frac{(x - m_{\mathrm{n}})^2}{2\sigma_{\mathrm{n}}^2}\right) . \tag{3.29}$$

The standard deviation σ_{n} again can be interpreted as the extent of the nuclide dispersion at time t in terms of distance. Since the compartment model and the continuum model should represent the same physical phenomenon, values of the extent of the dispersion should be the same. By equating $\sigma_{\mathrm{p}} L$ and σ_{n}, we obtain

$$L = 2D/v . \tag{3.30}$$

Since the dispersion coefficient D is associated with the longitudinal dispersivity α as

$$D = \alpha v ,$$

we obtain

$$L = 2\alpha . \tag{3.31}$$

Thus, the length of the aquifer compartments are determined as twice the value of the longitudinal dispersivity.

4 Benchmark Test of the Numerical Code

In this section we shall examine the difference between VR-KHNP model and SAGE model, show how these two different codes can solve the same problem, and compare the two sets of numerical results of the same problem.

4.1 Differences between VR-KHNP Model and SAGE Model

Infiltration Rate of Water in the Unsaturated Zone In SAGE, water infiltration rate can be described as a linear function or a piecewise step function. In VR-KHNP, only a piecewise step function can be assigned to the infiltration rate. Thus, in order to have SAGE perform the same calculation as VR-KHNP, a piecewise step function must be used.

Nuclide Release Mode from the Waste Form In VR-KHNP, it is assumed that all radionuclides in the waste form instantaneously dissolve in the groundwater at time $t = 0$. In SAGE, a fraction of the radionuclide in the waste instantaneously dissolves in the groundwater, and the rest dissolves congruently. The VR-KHNP assumption (i.e., 100% instant dissolution) corresponds to the following case in SAGE:

$$f_{\text{inst}} = 1 \quad \text{and} \quad f_{\text{cong}} = 0\,,$$

where f_{inst} is the fraction that dissolves instantaneously, and f_{cong} is the fraction that dissolves congruently.

Precipitation Precipitation is considered in SAGE. If the concentration of a nuclide in the water reaches its solubility limit, the excess amount of the nuclide in the compartment is stored in precipitate. The precipitate is considered immobile. On the other hand in VR-KHNP, precipitation is not considered. Nuclide concentration in the groundwater can reach a high value without solubility limit. Assigning the solubility to a sufficiently high value will prevent occurrence of precipitation in the SAGE calculation and thus will produce the same condition as in VR-KHNP.

Molecular Diffusion The effect of molecular diffusion is negligibly small compared to advection in the present study for the given parameter set. This is confirmed by calculating the Peclet number, which for the given parameter values is relatively large in all compartments at all times.

In SAGE, nuclide transport from a compartment to another due to molecular diffusion is formulated by means of the concentration difference and the diffusive mass transfer coefficients $\left(\frac{D}{d}\right)_{i\to i+1}$ and $T_{i\to i+1}$. In VR-KHNP, the effect of molecular diffusion is neglected, although some extent of a dispersive effect is introduced by the assumed uniform concentration in a compartment and transport

through the series of such compartments. The VR-KHNP situation (i.e., transport without molecular diffusion) is reproduced in SAGE when the mass transfer coefficients $\left(\frac{D}{d}\right)_{i\to i+1}$ and $T_{i\to i+1}$ are set to zero.

Interface between the Unsaturated Zone and the Saturated Zone In VR-KHNP, the nuclide released from the unsaturated zone (UZ) soil compartment first enter the saturated zone (SZ) compartments below the waste vault. If the horizontal dimension of the waste vault is large, radionuclides can flow into more than one SZ compartments. After entering the SZ compartments, radionuclides flow through the SZ compartments below the vault and then through ones at far field. The interface between the SZ compartments below the waste vault and those at far field has been called near-field/far-field interface (NFI) in our study.

In SAGE, all the nuclide released from the UZ soil compartment flows into the first compartment of the SZ *at far field*. This interface between the UZ and the SZ is called NFI in SAGE. The SZ compartments directly below the waste vault are not considered.

For the purpose of the benchmark test, we can have VR-KHNP perform the same calculation as SAGE by setting the horizontal length of the waste region small enough in VR-KHNP so that the entire waste compartment sits above a single aquifer compartment. In such a case, the SZ compartment below the waste vault must be considered as the first far-field compartment, and the UZ-SZ interface must be considered as the NFI. The modification of the waste vault length will change the volumes of UZ compartments and therefore the nuclide concentrations in the UZ compartments. However, it does not affect the release rate from each compartment or the compartment-wise mass distribution since solubility limits are not considered in VR-KHNP.

Cross-sectional Area of the Plume in the Aquifer The cross-sectional area of the contaminated water plume in the aquifer increases as the water flows downstream in SAGE, whereas it is treated to be constant in VR-KHNP. The effect of this difference between SAGE and VR-KHNP will be observed in nuclide concentration since the volume of the SZ compartments are different. However, the cross-sectional area does not affect the release rates [mol/yr], and therefore the difference is not observable in the release rate if precipitation and molecular diffusion are avoided in SAGE by the aforementioned methods.

4.2 Input Data and Conditions for Numerical Comparison

Proposed conditions for the benchmark test are described here. The parameter values are based on the configuration Model A. Special conditions and interpretations are added to VR-KHNP calculation and SAGE calculation in order to have the two codes perform (practically) the same calculation.

The main conditions for the VR-KHNP calculation are as follows:

- Assign the length of the repository shorter than that of a single aquifer compartment (10 m).
- Locate the waste compartment 180 m away from GBI. This is done because the waste compartment should entirely sit above the first aquifer compartment, and the first aquifer compartment must be included in the length of the far field, 200 m.
- Flux at the UZ-SZ interface (i.e., release rate from the UZ soil compartment at the bottom) in VR-KHNP is comparable to the NFI flux in SAGE.

The conditions for the SAGE calculation are as follows:

- Use piecewise step function for infiltration rate.
- Set 100% instant dissolution; $f_{\text{inst}} = 1$ and $f_{\text{cong}} = 0$.
- Solubility must be set to a sufficiently high (imaginary) value.
- No molecular diffusion; $\left(\frac{D}{d}\right)_{i \to i+1} = 0$ and $T_{i \to i+1} = 0$.

Beside the conditions listed above, the calculations performed by VR-KHNP and by SAGE must use the same number of compartments and the same physical properties (e.g., porosity, sorption coefficient, etc.).

The VR-KHNP calculation and the SAGE calculation still retain a difference in the cross-sectional area of aquifer compartments. As mentioned earlier, this difference only affects the concentration in SZ compartments but not the release rates. The calculation results must be therefore compared in terms of the release rates.

Radionuclides and the decay chains considered in the calculation are listed in Table 4.1. The physical properties of radionuclides and the media used in the numerical calculation are listed in Tables 4.2 through 4.6. The Model A values are used for initial inventories and properties for the waste compartment. Numerical calculations have been performed to produce the nuclide release rate at the UZ-SZ interface in model A configuration. In the calculation, however, there are five UZ compartments including three UZ soil compartments of 1 m height, which is different from the number of UZ compartments discussed in Section 3.

The content of input file used in VR-KHNP for the benchmark test is listed in Appendix C.

4.3 Results of Numerical Comparison

The radionuclide release rate at the UZ-SZ interface for each decay chain has been obtained from the VR-KHNP calculation based on the conditions described in the previous section. The result is compared to the flux data at NFI of the SAGE calculation. This SAGE calculation satisfies the conditions listed in

Table 4.1 Radionuclides and Decay Chains Considered in the Numerical Demonstration

Radionuclides of Single Member Decay Chains
^{3}H, ^{14}C, ^{60}Co, ^{59}Ni, ^{63}Ni, ^{90}Sr, ^{94}Nb, ^{99}Tc, ^{129}I, ^{137}Cs
Multi-Member Decay Chains
$^{238}\text{U} \rightarrow {}^{234}\text{U} \rightarrow {}^{230}\text{Th} \rightarrow {}^{226}\text{Ra} \rightarrow {}^{210}\text{Pb} \rightarrow {}^{210}\text{Po}$
$^{238}\text{Pu} \rightarrow {}^{234}\text{U} \rightarrow {}^{230}\text{Th} \rightarrow {}^{226}\text{Ra} \rightarrow {}^{210}\text{Pb} \rightarrow {}^{210}\text{Po}$
$^{239}\text{Pu} \rightarrow {}^{235}\text{U} \rightarrow {}^{231}\text{Pa} \rightarrow {}^{227}\text{Ac}$

Table 4.2 Radioactive Decay Constants of Nuclides

Nuclide	Decay Constant [1/yr]	Nuclide	Decay Constant [1/yr]
^{3}H	5.59×10^{-02}	^{210}Pb	3.11×10^{-02}
^{14}C	1.21×10^{-04}	^{210}Po	1.83×10^{-00}
^{60}Co	1.32×10^{-01}	^{226}Ra	4.33×10^{-04}
^{59}Ni	9.19×10^{-06}	^{227}Ac	3.18×10^{-02}
^{63}Ni	7.22×10^{-03}	^{230}Th	9.00×10^{-06}
^{90}Sr	2.38×10^{-02}	^{231}Pa	2.11×10^{-05}
^{94}Nb	3.41×10^{-05}	^{234}U	2.83×10^{-06}
^{99}Tc	3.25×10^{-06}	^{235}U	9.85×10^{-10}
^{129}I	4.41×10^{-08}	^{238}U	1.55×10^{-10}
^{137}Cs	2.31×10^{-02}	^{238}Pu	7.90×10^{-03}
		^{239}Pu	2.88×10^{-05}

Table 4.3 Sorption Distribution Coefficients [7]

Element	Distribution Coefficient [m^3/kg]			
	Waste	Concrete	UZ Soil	Aquifer
H	0	0	0	0
C	$2.50 \times 10^{+00}$	$2.50 \times 10^{+00}$	5.00×10^{-03}	1.00×10^{-02}
Co	2.00×10^{-02}	2.00×10^{-02}	1.50×10^{-02}	$1.00 \times 10^{+00}$
Ni	2.00×10^{-02}	2.00×10^{-02}	4.00×10^{-01}	$1.00 \times 10^{+00}$
Sr	2.50×10^{-03}	2.50×10^{-03}	1.50×10^{-02}	2.00×10^{-02}
Nb	5.00×10^{-01}	5.00×10^{-01}	0	$1.00 \times 10^{+00}$
Tc	5.00×10^{-01}	6.00×10^{-01}	1.00×10^{-04}	$1.00 \times 10^{+02}$
I	6.00×10^{-04}	6.00×10^{-04}	1.00×10^{-03}	5.00×10^{-03}
Cs	2.50×10^{-04}	2.50×10^{-04}	3.00×10^{-01}	1.00×10^{-01}
Pb	$2.00 \times 10^{+00}$	$2.00 \times 10^{+00}$	0	$1.00 \times 10^{+02}$
Po	$2.00 \times 10^{+00}$	$2.00 \times 10^{+00}$	0	$1.00 \times 10^{+02}$
Ra	$2.00 \times 10^{+00}$	$2.00 \times 10^{+00}$	0	$1.00 \times 10^{+02}$
Ac	$2.00 \times 10^{+00}$	$2.00 \times 10^{+00}$	0	$1.00 \times 10^{+02}$
Th	$2.00 \times 10^{+00}$	$2.00 \times 10^{+00}$	0	$1.00 \times 10^{+02}$
Pa	$2.00 \times 10^{+00}$	$2.00 \times 10^{+00}$	0	$1.00 \times 10^{+02}$
U	$2.00 \times 10^{+00}$	$2.00 \times 10^{+00}$	0	$1.00 \times 10^{+02}$
Pu	$4.00 \times 10^{+00}$	$4.00 \times 10^{+01}$	0	$5.00 \times 10^{+00}$

Table 4.4 Darcy Velocity of Groundwater in the UZ and the SZ [7]

	Darcy Velocity [m/yr]		
	0–100 yr	100–500 yr	After 500 yr
Waste	3.5×10^{-4}	3.5×10^{-2}	3.5×10^{-1}
Concrete	3.5×10^{-4}	3.5×10^{-2}	3.5×10^{-1}
Soil	3.5×10^{-4}	3.5×10^{-2}	3.5×10^{-1}
Aquifer	$1.0 \times 10^{+1}$	$1.0 \times 10^{+1}$	$1.0 \times 10^{+1}$

Table 4.5 Properties of Media [7]

	Dimension* [m]	Porosity	Saturation	Material Density [kg/m^3]
Waste				
for Models A & B	8.2	0.12	0.5	2840
for Models C & D				
Zone1 (Type1)	8.2	0.3	0.5	2857
Zone2 (Type2)	8.2	0.12	0.5	2840
Zone3 (Type3)	8.2	0.12	0.5	2840
Zone4 (Type3)	8.2	0.12	0.5	2840
Concrete	0.5	0.12	0.5	2840
Soil	3.0	0.3	0.7	2571
Aquifer	40.0†	0.25	1.0	3333

∗ The dimension of a compartment is measured along the flow direction of groundwater.

† The dimension of an aquifer compartment is determined by Eq. (3.31).

Table 4.6 Initial Inventory [7]

Nuclide	Initial Inventory [Bq]				
	Models A & B	Models C & D			
		Zone1	Zone2	Zone3	Zone4
^{3}H	$2.67 \times 10^{+13}$	$2.97 \times 10^{+11}$	$9.20 \times 10^{+12}$	$0.86 \times 10^{+13}$	$0.86 \times 10^{+13}$
^{14}C	$1.68 \times 10^{+13}$	$2.67 \times 10^{+11}$	$1.66 \times 10^{+12}$	$0.75 \times 10^{+13}$	$0.75 \times 10^{+13}$
^{60}Co	$1.73 \times 10^{+14}$	$1.82 \times 10^{+13}$	$1.09 \times 10^{+14}$	$2.32 \times 10^{+13}$	$2.32 \times 10^{+13}$
^{59}Ni	$3.64 \times 10^{+12}$	$3.36 \times 10^{+11}$	$1.21 \times 10^{+12}$	$1.05 \times 10^{+12}$	$1.05 \times 10^{+12}$
^{63}Ni	$9.51 \times 10^{+13}$	$1.29 \times 10^{+13}$	$5.25 \times 10^{+13}$	$1.49 \times 10^{+13}$	$1.49 \times 10^{+13}$
^{90}Sr	$1.39 \times 10^{+12}$	$1.22 \times 10^{+11}$	$1.16 \times 10^{+12}$	$0.53 \times 10^{+11}$	$0.53 \times 10^{+11}$
^{94}Nb	$1.00 \times 10^{+11}$	$1.81 \times 10^{+10}$	$7.28 \times 10^{+10}$	$4.59 \times 10^{+09}$	$4.59 \times 10^{+09}$
^{99}Tc	$4.07 \times 10^{+10}$	$5.42 \times 10^{+09}$	$2.65 \times 10^{+10}$	$4.37 \times 10^{+09}$	$4.37 \times 10^{+09}$
^{129}I	$1.25 \times 10^{+10}$	$6.12 \times 10^{+08}$	$3.94 \times 10^{+09}$	$4.00 \times 10^{+09}$	$4.00 \times 10^{+09}$
^{137}Cs	$6.09 \times 10^{+13}$	$6.70 \times 10^{+12}$	$5.24 \times 10^{+13}$	$0.93 \times 10^{+12}$	$0.93 \times 10^{+12}$
^{210}Pb	0	0	0	0	0
^{210}Po	0	0	0	0	0
^{226}Ra	0	0	0	0	0
^{227}Ac	0	0	0	0	0
^{230}Th	0	0	0	0	0
^{231}Pa	0	0	0	0	0
^{234}U	0	0	0	0	0
^{235}U	$1.91 \times 10^{+08}$	$4.49 \times 10^{+06}$	$3.61 \times 10^{+07}$	$0.75 \times 10^{+08}$	$0.75 \times 10^{+08}$
^{238}U	$4.75 \times 10^{+10}$	$1.32 \times 10^{+10}$	$3.40 \times 10^{+10}$	$1.72 \times 10^{+08}$	$1.72 \times 10^{+08}$
^{238}Pu	$1.28 \times 10^{+11}$	$2.75 \times 10^{+09}$	$3.89 \times 10^{+10}$	$4.31 \times 10^{+10}$	$4.31 \times 10^{+10}$
^{239}Pu	$5.89 \times 10^{+10}$	$5.23 \times 10^{+09}$	$4.08 \times 10^{+10}$	$0.65 \times 10^{+10}$	$0.65 \times 10^{+10}$

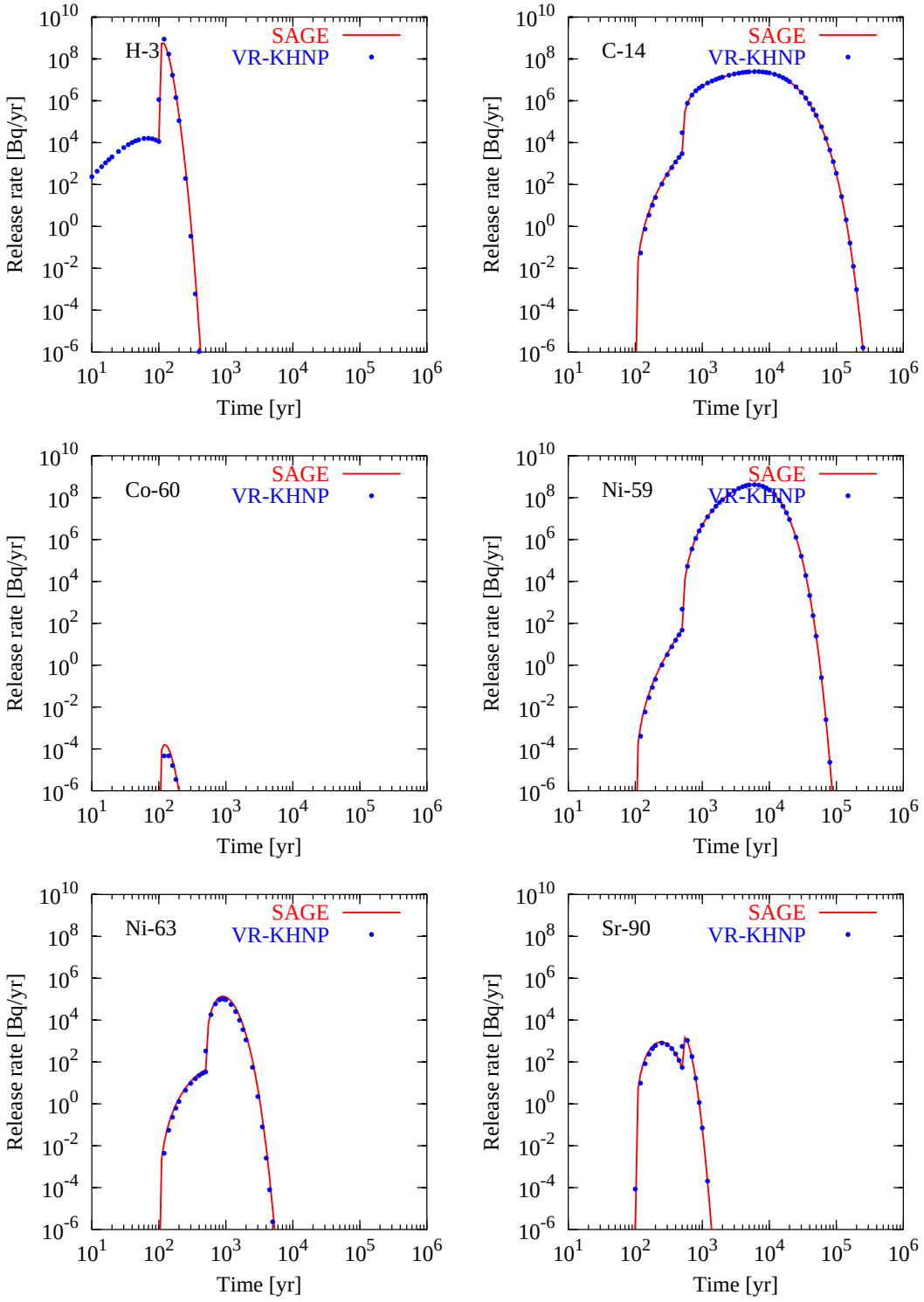

Figure 4.1 Results of benchmark test: release rates at UZ-SZ interface calculated by VR-KHNP (dots) and by SAGE (solid curves).

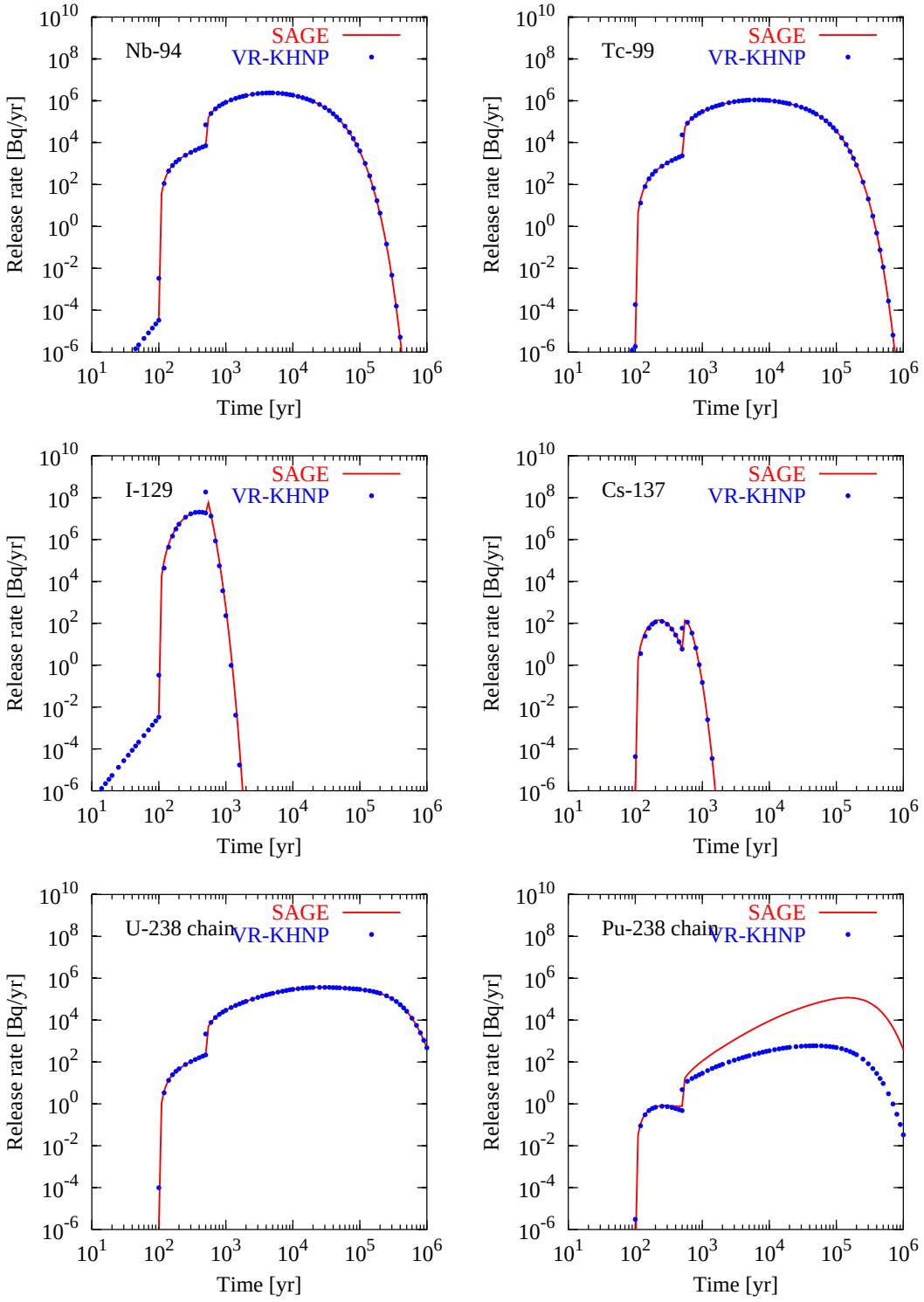

Figure 4.2 Results of benchmark test: release rates at UZ-SZ interface calculated by VR-KHNP (dots) and by SAGE (solid curves).

Section 4.2 with exception regarding molecular diffusion. However, the effect of molecular diffusion is estimated to be negligibly small as mentioned earlier.

The release rates are plotted in Figures 4.1, 4.2, and 4.3. It is observed that the results of the VR-KHNP calculation and those of SAGE agree well with each other for all nuclides except for the ^{238}Pu chain.

The reason for the difference in the ^{238}Pu-chain release rate is considered as follows: In the calculation used for the benchmark test, the ^{238}U chain and ^{238}Pu chain share the same daughter nuclides such as ^{234}U, ^{230}Th, ^{226}Ra, etc. In SAGE, all the decay chains are calculated together, and the release rate of ^{234}U, for example, is calculated as the sum of the release rate of ^{234}U as a daughter of ^{238}Pu and ^{234}U as a daughter of ^{238}U. The daughter nuclide in two different chains is not separated. Thus the release rate of all the ^{238}Pu chain members obtained from SAGE contains the contribution from the daughter nuclides in the ^{238}U chain. In VR-KHNP, on the other hand, the decay chains are calculated separately. The release rate of ^{234}U in the ^{238}Pu chain is distinguished from that of ^{234}U in the ^{238}U chain. The release rate of all the ^{238}Pu chain members obtained from VR-KHNP does not contain the contribution from the daughter nuclides in the ^{238}U chain.

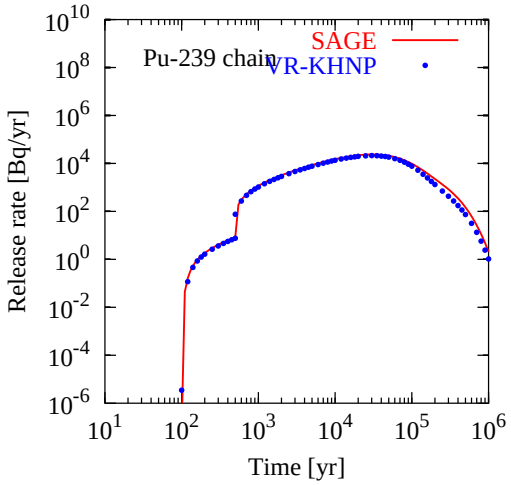

Figure 4.3 Results of benchmark test: release rates at UZ-SZ interface calculated by VR-KHNP (dots) and by SAGE (solid curves).

5 Numerical Investigation with VR-KHNP

5.1 Configuration Models and Input Data

Four different geometry models are considered in order to reflect the differences in groundwater orientation and in the level of geometry simplification. Structure and the dimensions of each geometry model are shown in Figure 5.1.

Models A and B contain a single waste compartment, in which all the radionuclides are initially contained. Models C and D contain four separate waste compartments (zones 1, 2, 3, and 4) to reflect the detailed heterogeneity of the repository. There are three types of waste having different inventories and properties (see Tables 4.5 and 4.6). In Models C and D, Type-1 waste is put into Zone 1, Type-2 into Zone 2, and Type 3 into Zones 3 and 4. In Models A and B, the single waste compartment contains the waste of all types homogenized over the compartment volume. The essential difference between Models A and B (and also between Models C and D) is the groundwater flow orientation in the aquifer relative to the waste vault orientation. The initial inventory of each radionuclide in the entire repository is the same for all four configuration models.

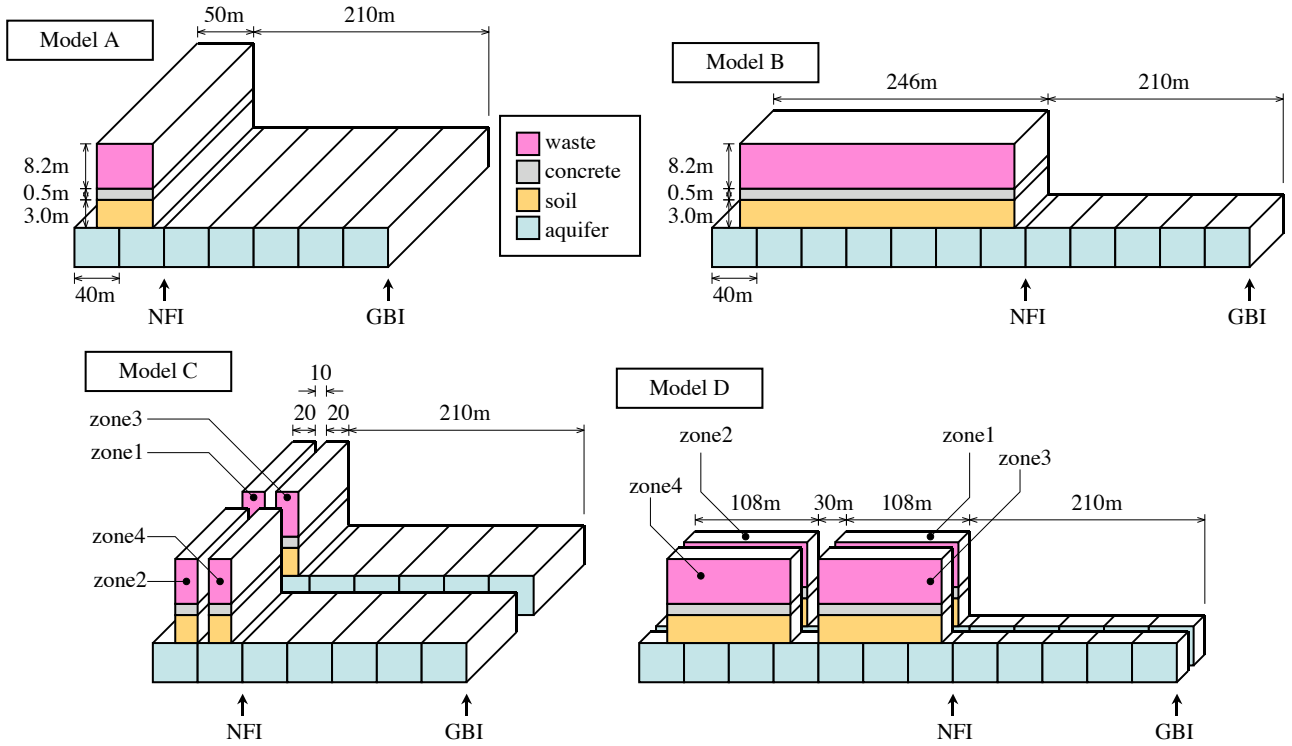

Figure 5.1 Schematic diagrams of four configuration models and compartment arrangement.

Table 5.1 Maximum permissible concentration (MPC) of radionuclides [9].

Nuclide	MPC [Ci/m^3]	Nuclide	MPC [Ci/m^3]
^{3}H	1×10^{-3}	^{238}Pu	2×10^{-8}
^{14}C	3×10^{-5}	^{238}U	3×10^{-7}
^{60}Co	3×10^{-6}	^{234}Pa	3×10^{-5}
^{59}Ni	3×10^{-4}	^{234}U	3×10^{-7}
^{63}Ni	1×10^{-4}	^{230}Th	1×10^{-7}
^{90}Sr	5×10^{-7}	^{226}Ra	6×10^{-8}
^{94}Nb	1×10^{-5}	^{214}Pb	1×10^{-4}
^{99}Tc	6×10^{-5}	^{214}Bi	3×10^{-4}
^{129}I	2×10^{-7}	^{210}Pb	1×10^{-8}
^{137}Cs	1×10^{-6}	^{210}Bi	1×10^{-5}
^{239}Pu	2×10^{-8}	^{210}Po	4×10^{-8}
^{235}U	3×10^{-7}		
^{231}Pa	6×10^{-9}		
^{227}Ac	5×10^{-9}		
^{227}Th	2×10^{-6}		
^{223}Ra	1×10^{-7}		
^{211}Pb	2×10^{-4}		

Radionuclides and the decay chains considered in the calculation are listed in Table 4.1. Some short-lived radionuclides in the multi-member decay chains are omitted. For example ^{238}U is treated as if it directly decays into ^{234}U, skipping intermediate nuclides ^{234}Th and ^{234}Pa. The omitted nuclides are assumed to be at secular equilibrium with their parent nuclide all the times. Parameter values used in the calculations are listed in Tables 4.2 through 4.6. The MPC values used for obtaining toxicity indices are listed in Table 5.1.

Based on these input parameter values, average lifetimes of radionuclides and average residence times in compartments are obtained and are listed in Table 5.2. For the residence times in UZ compartments, only the ones in Model A after 500 yr are shown. Average residence times before 500 yr are readily estimated by observing these residence times and the Darcy velocity shown in Table 4.4 since the average residence time is inversely proportional to Darcy velocity.

It is observed that, because of zero sorption of H, the residence times of ^{3}H are siginificantly shorter than other nuclides. The residence time of ^{14}C in the UZ compartments is observed significantly greater than that in an aquifer compartment, while for other nuclides, magnitude of residence times in the UZ compartments is comparable to or less than those in an aquifer compartment.

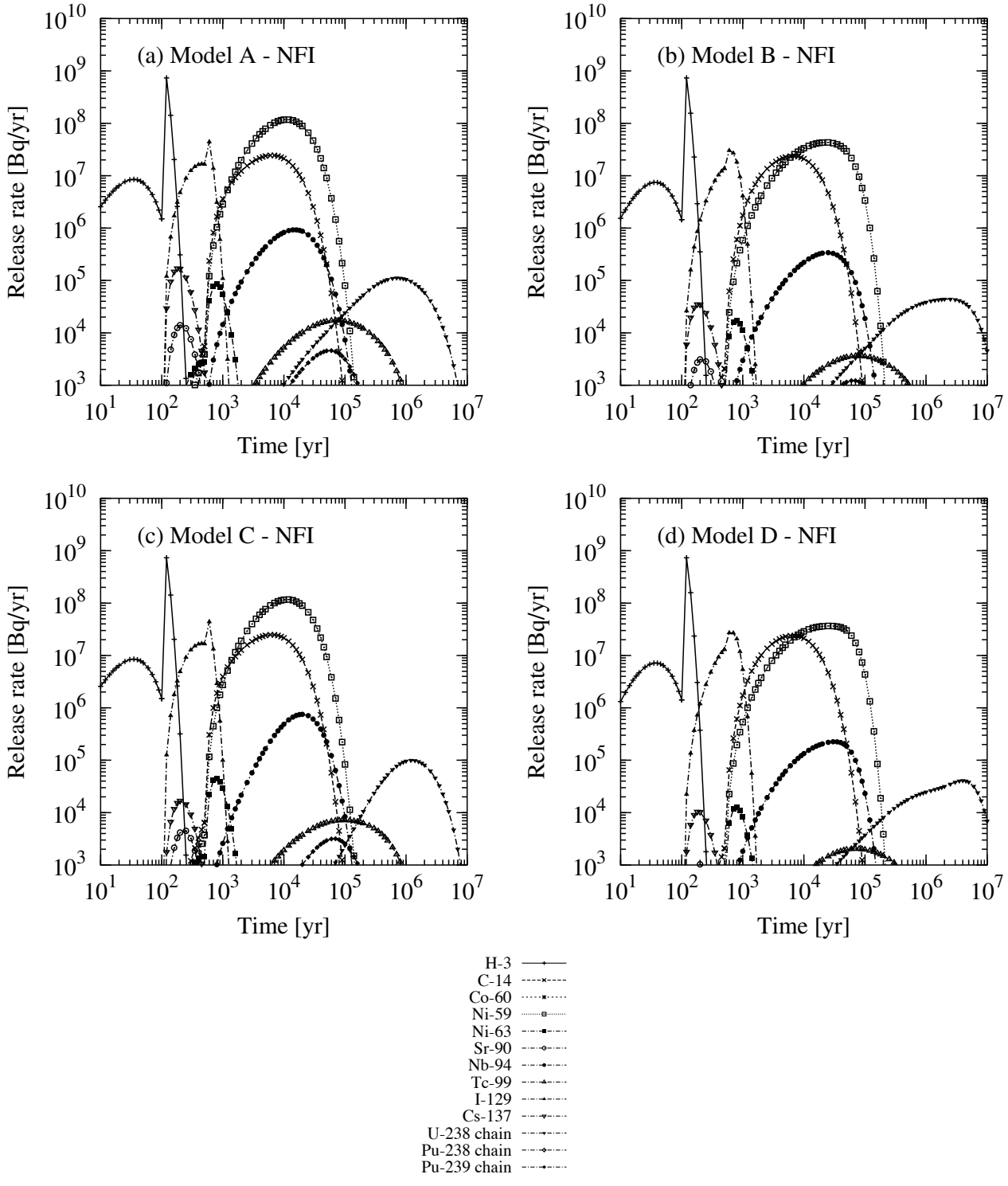

Figure 5.2 Release rates of radionuclides at the NFI for four configuration models.

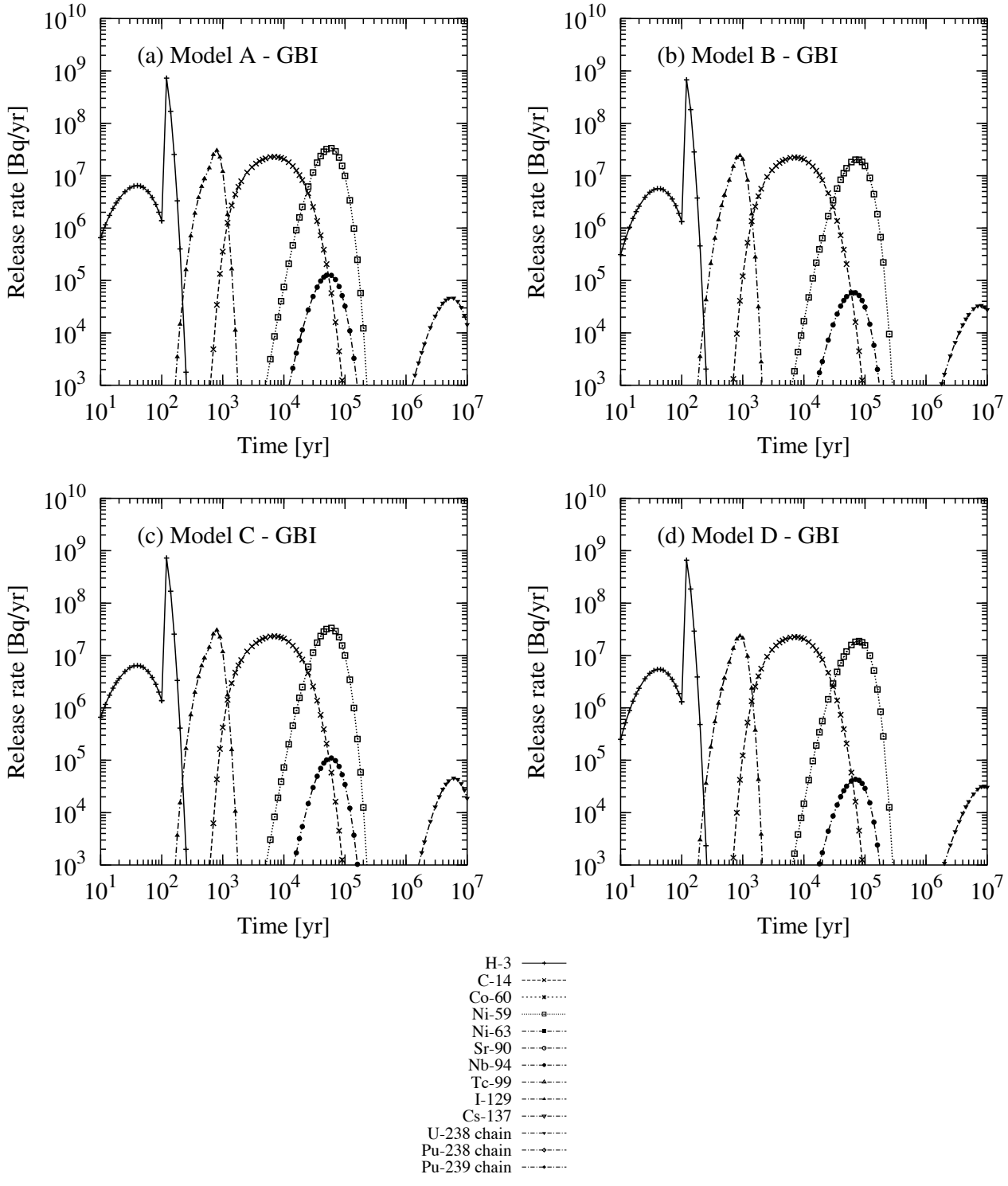

Figure 5.3 Release rates of radionuclides at the GBI for four configuration models.

Table 5.2 Average Lifetime of Radionuclides and Average Residence Times in Compartments

Nuclide	Ave. Lifetime	Ave. Res. Time		
		Entire UZ ($t > 500\,\mathrm{yr}$)†	Aquifer*	
	$1/\lambda^{(i)}$	$\sum_{m=1}^{3} 1/\mu_{k,l,m}^{(i)}$	$1/\mu_{\mathrm{SZ}}^{(i)}$	$\lambda^{(i)}/\mu_{\mathrm{SZ}}^{(i)}$
^{3}H	$1.79 \times 10^{+01}$	$3.29 \times 10^{+00}$	$1.00 \times 10^{+00}$	5.59×10^{-02}
^{14}C	$8.26 \times 10^{+03}$	$1.55 \times 10^{+05}$	$1.01 \times 10^{+02}$	1.22×10^{-02}
^{60}Co	$7.58 \times 10^{+00}$	$1.48 \times 10^{+03}$	$1.00 \times 10^{+04}$	$1.32 \times 10^{+03}$
^{59}Ni	$1.09 \times 10^{+05}$	$7.42 \times 10^{+03}$	$1.00 \times 10^{+04}$	9.19×10^{-02}
^{63}Ni	$1.38 \times 10^{+02}$	$7.42 \times 10^{+03}$	$1.00 \times 10^{+04}$	$7.22 \times 10^{+01}$
^{90}Sr	$4.20 \times 10^{+01}$	$3.90 \times 10^{+02}$	$2.01 \times 10^{+02}$	$4.78 \times 10^{+00}$
^{94}Nb	$2.93 \times 10^{+04}$	$3.11 \times 10^{+04}$	$1.00 \times 10^{+04}$	3.41×10^{-01}
^{99}Tc	$3.08 \times 10^{+05}$	$3.14 \times 10^{+04}$	$1.00 \times 10^{+06}$	$3.25 \times 10^{+00}$
^{129}I	$2.27 \times 10^{+07}$	$5.60 \times 10^{+01}$	$5.10 \times 10^{+01}$	2.25×10^{-06}
^{137}Cs	$4.33 \times 10^{+01}$	$4.65 \times 10^{+03}$	$1.00 \times 10^{+03}$	$2.31 \times 10^{+01}$
^{210}Pb	$3.22 \times 10^{+01}$	$1.24 \times 10^{+05}$	$1.00 \times 10^{+06}$	$3.11 \times 10^{+04}$
^{210}Po	5.46×10^{-01}	$1.24 \times 10^{+05}$	$1.00 \times 10^{+06}$	$1.83 \times 10^{+06}$
^{226}Ra	$2.31 \times 10^{+03}$	$1.24 \times 10^{+05}$	$1.00 \times 10^{+06}$	$4.33 \times 10^{+02}$
^{227}Ac	$3.14 \times 10^{+01}$	$1.24 \times 10^{+05}$	$1.00 \times 10^{+06}$	$3.18 \times 10^{+04}$
^{230}Th	$1.11 \times 10^{+05}$	$1.24 \times 10^{+05}$	$1.00 \times 10^{+06}$	$9.00 \times 10^{+00}$
^{231}Pa	$4.74 \times 10^{+04}$	$1.24 \times 10^{+05}$	$1.00 \times 10^{+06}$	$2.11 \times 10^{+01}$
^{234}U	$3.53 \times 10^{+05}$	$1.24 \times 10^{+05}$	$1.00 \times 10^{+06}$	$2.83 \times 10^{+00}$
^{235}U	$1.02 \times 10^{+09}$	$1.24 \times 10^{+05}$	$1.00 \times 10^{+06}$	9.85×10^{-04}
^{238}U	$6.45 \times 10^{+09}$	$1.24 \times 10^{+05}$	$1.00 \times 10^{+06}$	1.55×10^{-04}
^{238}Pu	$1.27 \times 10^{+02}$	$3.77 \times 10^{+05}$	$5.00 \times 10^{+04}$	$3.95 \times 10^{+02}$
^{239}Pu	$3.47 \times 10^{+04}$	$3.77 \times 10^{+05}$	$5.00 \times 10^{+04}$	$1.44 \times 10^{+00}$

∗ Average residence time in a single aquifer compartment is shown.

† Values are for UZ compartments in Model A.

5.2 Release Rates at the NFI and the GBI

The release rates of radionuclides at NFI and at GBI for each configuration model, obtained with the mathematical model and the parameter values mentioned earlier, are plotted in Figures 5.2 and 5.3. For a multi-member decay chain, the sum of the release rates for all member nuclides is plotted.

In all configuration models, ^{3}H is released at very early times, and other elements with low sorption coefficients, such as I and Cs, follow. Release of U, Pu, and their daughter nuclides is delayed because of the assumed high sorption in the aquifer.

5.2.1 Effects of Groundwater Flow Direction

Comparison between Figures 5.2(a) and 5.2(b) shows that the peak of the release rate at NFI in Model A is observed earlier than that in Model B for some nuclides (e.g., ^{59}Ni and ^{94}Nb), and that the magnitude of the peak in Model A is higher for some radionuclides (e.g., ^{63}Ni, ^{99}Tc, and ^{137}Cs). It is observed, however, the release rate profiles for ^{3}H and ^{14}C have little difference between Models A and B.

As mentioned earlier, the difference between Models A and B is the groundwater flow direction in the saturated zone. There is no difference in the unsaturated zone compartments between these two models. In the present mathematical model, radionuclide distribution in the unsaturated zone is not affected by the properties in the saturated zone. Therefore, the flux of radionuclides at any point in the unsaturated zone is identical between Model A and Model B. The difference in the release rates at NFI between these two models is due to the difference in times spent for nuclide migration in the aquifer before the nuclide reaches NFI, which can be represented by the product of $1/\mu_{\mathrm{SZ}}^{(i)}$ and the number of aquifer compartments that the nuclide migrates through.

Since the series of aquifer compartments in Model A are shorter than those in Model B, nuclides spend a shorter time in aquifer in Model A. Therefore, the peaks of release rates at NFI are observed later in Model B than in Model A, and, if the nuclide has a relatively short half-life compared to the time spent in the aquifer, the magnitude of the peak is observed lower in Model B because of radioactive decay inside the aquifer compartments.

Another aspect of this difference is that the residence time in the near-field aquifer compartments is more spread in Model B. The radionuclide released into the aquifer far away from the NFI takes more time to reach the NFI than one relased into the aquifer near the NFI. This deviation is greater in Model B than in Model A. It follows that the release of a nuclide in Model B is more spread over time, and the peak of its release rate is lower than in Model A.

Because of these effects, peaks of the release rates are observed later and lower in Model B for ^{59}Ni and ^{94}Nb, which have relatively long half-lives and great sorption coefficient in the aquifer.

The short-lived radionuclides with high sorption coefficients in the aquifer, such as ^{63}Ni, ^{90}Sr, and ^{137}Cs, show lower release rate in Model B. However, little difference is observed in the duration of release.

This is because the release of these nuclides is limited by radioactive decay.

For ^{3}H, ^{14}C, and ^{129}I, the residence time in an aquifer compartment, $1/\mu^{(i)}_{\mathrm{SZ}}$, is so short compared to those in the unsaturated zone, $1/\mu^{(i)}_{k,l,1} + 1/\mu^{(i)}_{k,l,2} + 1/\mu^{(i)}_{k,l,3}$, (because of the relatively small sorption distribution coefficient and fast water velocity in the aquifer) that the difference in the residence times in aquifer compartments is not significant.

The above discussion also applies to the comparison between the release rates in Model C and in Model D.

5.2.2 Effect of Heterogeneity

There is one waste region in Model A, in which the radionuclides are uniformly distributed. Model A is considered as a simplified version of Model C which has more detailed geometry of four waste regions with heterogeneous distribution of radionuclides. It is of our interest to investigate whether the simplified Model A reproduces the release rates in Model C.

Comparison of the release rates at NFI between Models A and C shows that there is little difference for ^{3}H, ^{14}C, and ^{129}I. Since these nuclides have relatively short residence time in aquifer compartments, the heterogeneous distribution of nuclide source has little effect on the release rate at the NFI.

On the other hand, ^{90}Sr, ^{94}Nb, ^{137}Cs, and ^{63}Ni have lower release rate in Model C than in Model A. Sorption in the aquifer for these nuclides is relatively greate, and hence the residence time in the aquifer is so significant that location of the nuclide source affects the release rate at the NFI. Most of these nuclides are initially contained in zone 2 (which is upstream side of the repository) in Model C. This results in a longer residence time in the near-field aquifer compartments.

The same discussion applies to the comparison between Models B and D.

5.2.3 Release Rates at GBI

Figure 5.3 shows that only ^{3}H, ^{14}C, ^{59}Ni, ^{94}Nb, ^{129}I, and ^{238}U chain have siginificant magnitude of radioactivity release at GBI. These radionuclides have relatively long half-lives compared to the time spent for migration and thus survive until they reach GBI. Other radionuclides, such as ^{63}Ni and ^{137}Cs, have relatively short half-lives and mostly decay out before they reach GBI.

5.3 Attenuation Effect in the Aquifer at Far Field

The 200 m distance between NFI and GBI has been arbitrarily chosen for the demonstration in the present study. This distance, however, has important effects as a natural barrier between the source of radionuclides and the environment:

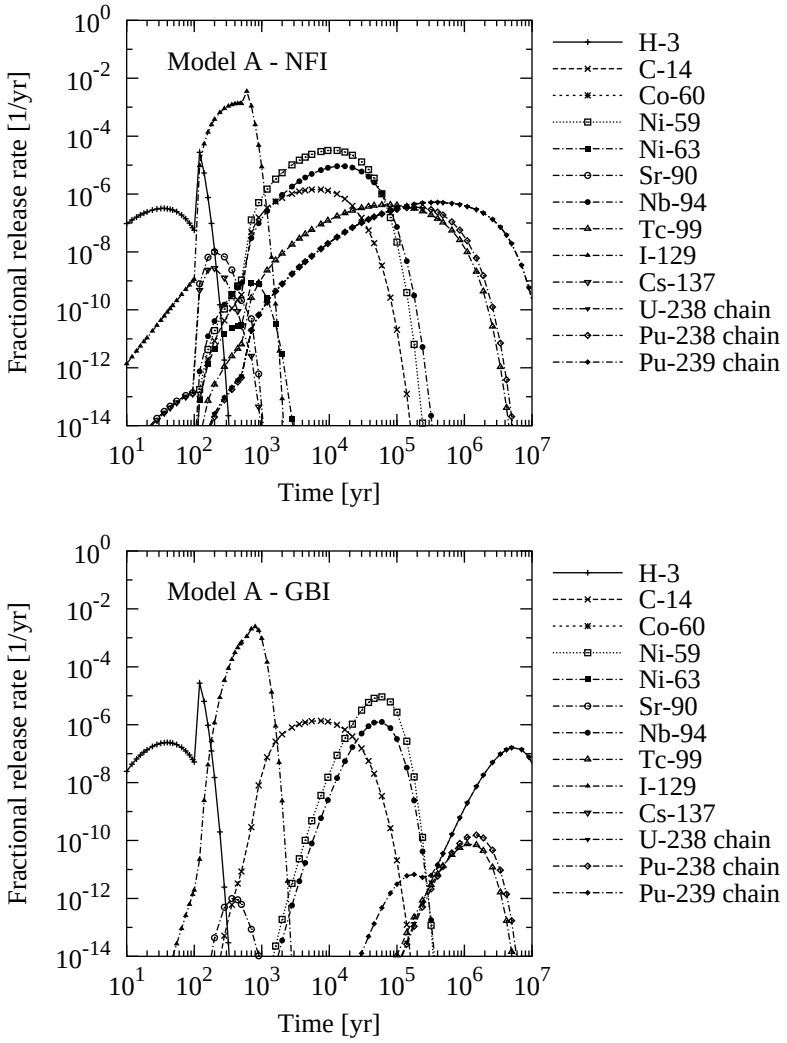

Figure 5.4 Fractional release rates at NFI and at GBI in configuration model A. Fractional release rate is the release rate normalized to the initial inventory of the nuclide and is defined in Eqs. (3.20) and (3.21).

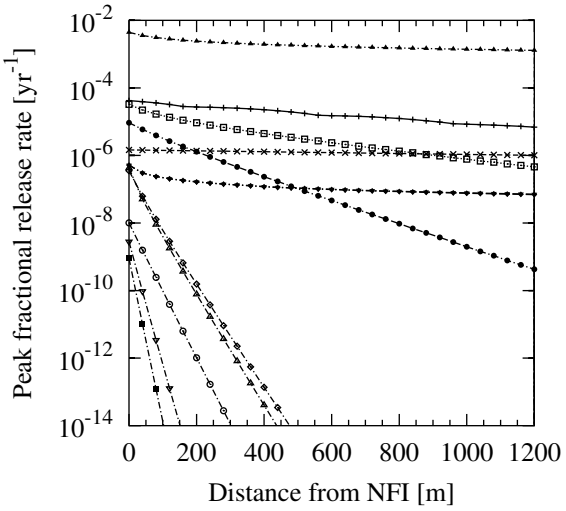

Figure 5.5 Peak fractional release rates of radionuclides at various points at far field.

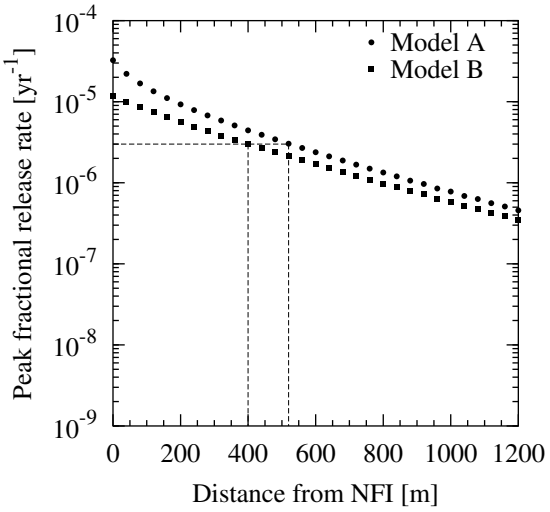

Figure 5.6 Peak fractional release rates of ^{59}Ni in Models A and B.

- Radionuclides undergo radioactive decay while they migrate through the far-field aquifer region, and therefore the amount of radionuclides released through GBI is somewhat less than that through NFI. Thus, there is an attenuation effect on radionuclide flux over the distance.

- Some short-lived radionuclides can attenuate significantly in the far-field aquifer region. From the viewpoint of performance assessment, the number of radionuclides of concern can be significantly reduced by properly allocating this distance.

We can consider GBI as the borders of the site in which the LLW repository will be located, because the site borders will still be maintained after the waste emplacement. In such case, the region exterior to the site is considered as the environment, and the aquifer within the site is a natural barrier.

The attenuation effect in radionuclide release due to radioactive decay can be explained with the fractional release rates defined in Eq. (3.20). The fractional release rates at NFI and GBI for Model A are plotted in Figure 5.4. Majority of ^{63}Ni, ^{90}Sr, and ^{137}Cs decay before they reach NFI, and their fractional release rates at NFI are observed significantly low. These nuclides decay further in the far-field aquifer, and the fractional release rates at GBI are even lower.

Other nuclides, such as ^{59}Ni and ^{129}I, survive until they reach NFI and GBI. While there is no siginificant reduction due to radioactive decay for ^{99}Tc observed at NFI, the peak level of its fractional release rate at GBI is significantly lower than that at NFI. This is because its residence time in aquifer compartments is longer than its average life time $1/\lambda^{(i)}$, while the residence time in the UZ is shorter than $1/\lambda^{(i)}$ for ^{99}Tc (see Table 5.2).

Figure 5.5 shows the peak value of the fractional release rate for each radionuclide as a function of the distance from the NFI. This result has been obtained by extending the array of far-field aquifer compartments to the point 1200 m away from NFI in the downstream direction. The release rates have been obtained for each compartment in the aquifer. In the plot, 0 m and 200 m points correspond to the NFI and the GBI for Model A, respectively. Note that the time of the peak is different for each location and each radionuclide.

Attenuation of radionuclides is observed as the decreasing values of the peak fractional release rate. There are two reasons for this decrease; one is radioactive decay and the other is spatial dispersion effect in the aquifer.

The rate of decrease is remarkable for some short-lived radionuclides, such as ^{63}Ni, ^{90}Sr, and ^{137}Cs. Since the characteristic time of migration over the distance of x [m] is written as $x/\mu_{\mathrm{SZ}}^{(i)}l$, the slope of this curve can be characterized by $\exp[\lambda^{(i)}x/\mu_{\mathrm{SZ}}^{(i)}l]$, where x is the distance of the location from NFI, and l is the length of one aquifer compartment. The ratio $\lambda^{(i)}/\mu_{\mathrm{SZ}}^{(i)}$ is listed in the last column of Table 5.2. A greater value of this ratio means that the radionuclide attenuates more by radioactive decay during the time it moves a fixed distance. The aforementioned short-lived radionuclides have relatively great values of this ratio. However, it is observed in Figure 5.5 that the peak release rate of ^{3}H does not decrease as much even though it has a short half-life. This is due to the shorter residence time in the aquifer compartments, which

leads to the small value of the ratio $\lambda^{(i)}/\mu_{SZ}^{(i)} = 5.59 \times 10^{-2}$. In the contrast, relatively long-lived ^{99}Tc shows significant decrease due to radioactive decay, having a long residence time in aquifer compartments.

^{129}I has a small ratio $\lambda^{(i)}/\mu_{SZ}^{(i)}$ and there is little contribution of radioactive decay to the decrease in peak release rate. The decrease over the distance is mainly due to dispersion effect during migration. The effect of dispersion on the peak is greater in a short distance, and becomes less and less for longer distance.

The peak release rate for ^{14}C shows very little decrease over 1200 m. The effect of radioactive decay is very small during the migration time. The effect of dispersion for ^{14}C is not significant because its release rate at NFI has a broad peak which spans over a time duration much longer than its residence time in the aquifer.

By assigning proper borders of the repository site, the peak release rates from the site can be significantly reduced for nuclides such as ^{63}Ni, ^{90}Sr, ^{99}Tc, ^{137}Cs, and ^{238}Pu decay chain members. On the other hand, increase in the distance between NFI and the site border does not introduce much reduction effect on peak release rate of ^{3}H, ^{14}C, ^{129}I, ^{238}U decay chain members, and ^{239}Pu decay chain members.

Figure 5.6 shows the peak fractional release rate of ^{59}Ni for Models A and B. Release rate for Model B is lower than that for Model A at all locations because effects of radioactive decay and dispersion in the near-field aquifer compartments are greater for the Model B. If, for example, a regulation limits the maximum fractional release rate of ^{59}Ni at the border of the site to $3 \times 10^{-6}\,\mathrm{yr}^{-1}$, the border must be at least 520 m distant from NFI for Model A while it must be at least 400 m distant for Model B. This also implies that if the site borders arround the reopsitory are more than 520 m away from two edges of the waste vault and more than 400 m away from the other two edges, then it meets the regulation requirement regardless of the groundwater flow direction in the aquifer.

5.4 Variable Infiltration Rate and Constant Infiltration Rate

In this section, we shall investigate the importance of change in Darcy velocity in the early times. Figure 5.7 shows the radionuclide release rates for Model A with a constant Darcy velocity 0.35 m/yr for all time in the UZ compartments instead of lower Darcy velocities in the early times shown in Table 4.4.

Comparing Figure 5.2 and Figure 5.7, the peak release rates of short-lived radionuclides (^{3}H, ^{60}Co, ^{63}Ni, ^{90}Sr, ^{137}Cs) at NFI in the latter are significantly greater than those in the former. Other nuclides such as ^{59}Ni and ^{14}C start being released earlier in the latter, although the magnitude of the peak is not affected.

It is observed in Figure 5.7 that most of the short-lived nuclides still decay out during migration in the aquifer, and thus their release rates at GBI are not significant except for ^{3}H which moves through aquifer very quickly. The peak of ^{129}I has shifted earlier. Peaks of other nuclides (^{14}C, ^{59}Ni, ^{94}Nb, and ^{238}U decay chain members) at GBI are not affected by the Darcy velocity difference during the early times.

5.5 Environmental Impact

The radiotoxicity index of each radionuclide in the environment is shown in Figure 5.8. It shows that environmental impact of the LLW repository is dominated by ^{129}I at the early times (from around 300 years until 10^6 yr). After 10^6 yr, toxicities of ^{238}U and its daughters become significant. By this time, all the daughter nuclides of ^{238}U have reached a secular equilibrium and have the same radioactivity as ^{238}U. The highest toxicity is marked by ^{210}Pb, which has the lowest MPC level. Because of the long half-lives of these nuclides, almost all the amount of ^{129}I and ^{238}U initially emplaced in the repository will be eventually released into the environment before they undergo radioactive decay. In order to reduce contributions of these radionuclides to the environmental impact, we therefore need to reduce the initial inventories of these radionuclides in the repository.

The repository performance assessment in the present study is based on the assumption that the repository contains 400,000 drums of 200-liter capacity. Assuming that an average number of drums that are generated from 1 GWyr in terms of electricity generation supported by this repository. From Figure 5.8, the peak environmental impact from the repository is about 10^8 m^3. From these values, the environmental impact of the repository per unit electricity generation is estimated as 2.5×10^5 m^3/GWyr.

Let us consider the environmental impacts from other waste sources for comparison. The level of the environmental impact of the mill talings and depleted uranium generated by an LWR is of the order of 10^{10} m^3/GWyr.

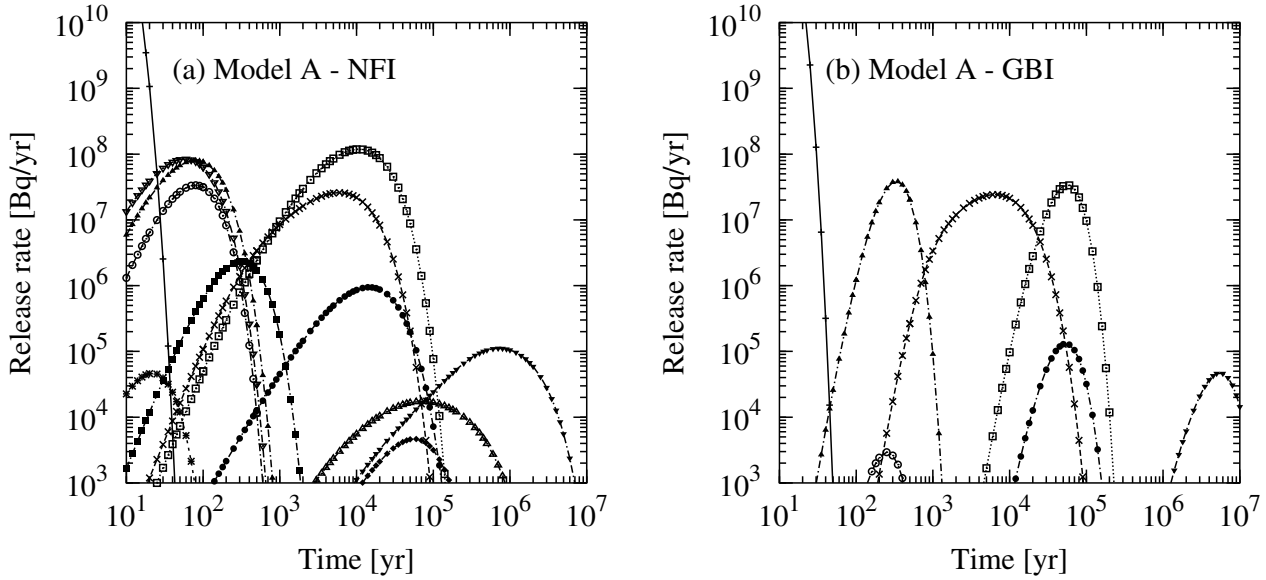

Figure 5.7 Release rates at NFI (a) and at GBI (b) in Model A calculated with constant Darcy velocity 0.35 m/yr in the UZ. The other parameter values are identical to those used for Figures 5.2 and 5.3. Refer to Figure 5.2 for legends.

For a high-level waste repository, we consider two examples: the Yucca Mountain Repository (YMR) and the H12 conceptual repository being developed in Japan. The former exemplifies the case with the spent-fuel direct disposal in a water-unsaturated repository, whereas the latter the case with vitrified reprocessed waste disposed of in a water saturated repository. The environmental impact from the YMR is at the level of 1.6×10^9 m^3/GWyr, mainly due to ^{237}Np and ^{238}U and its decay daughters [10]. The contributions of these nuclides are nearly equal to each other. The environmental impact of the H12 repository was evaluated to be of the order of 5×10^7 m^3/GWyr [8]. The impact of H12 repository is smaller than that of YMR because most of uranium and plutonium is removed from the spent fuel when HLW is vitribied and the geochemical environment assumed in H12 is more favorable for neptunium confinement than that in YMR.

Compared with these values, it can be said that the environmental impact of the proposed LLW repository by KHNP is smaller than the H12 high-level waste repository by a factor of 200.

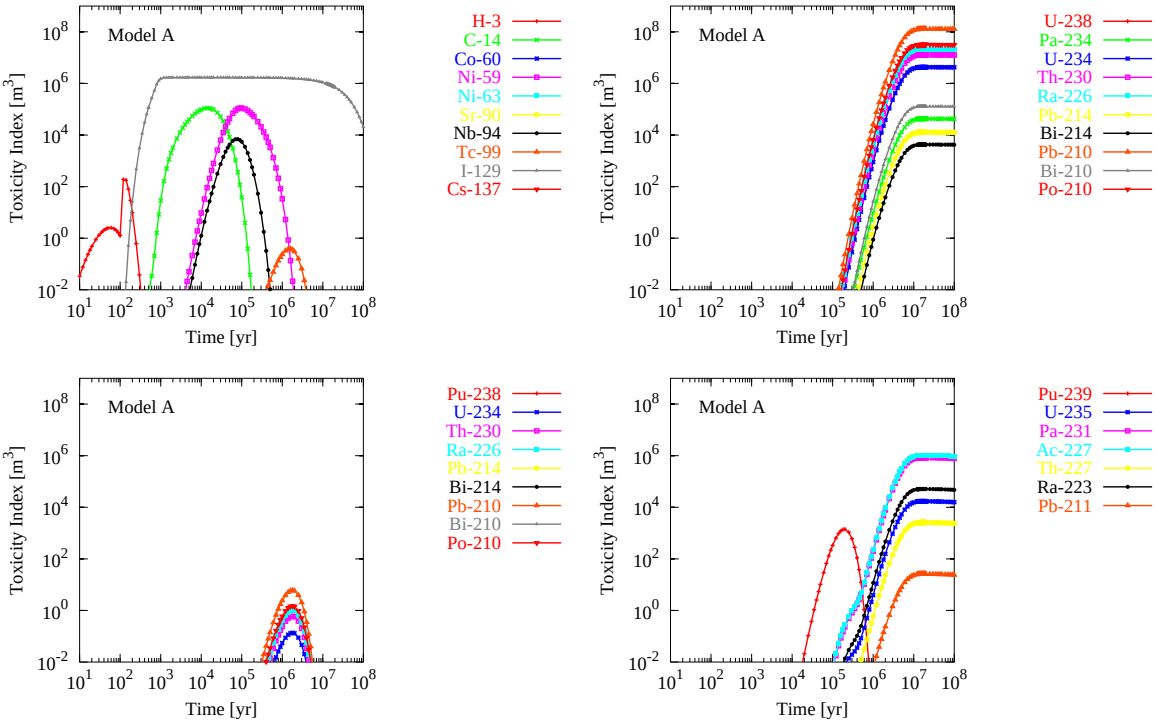

Figure 5.8 Toxicity indices in the environment.

6 Conclusion

A compartment model has been developed for radionuclide transport through the groundwater at LLW repository site. The VR-KHNP code calculates mass, flux, and concetration of a radionuclide in each compartment as functions of time. It models radionuclide transport through the EBS, UZ, and aquifer at near field and at far field, taking into account multi-member decay chain, arrangement and dimensions of the waste form, and water infiltration rate change with time.

Benchmark test of the numerical code has been made for VR-KHNP by comparing results with those from the existing SAGE code in a special condition. The two results have shown good agreement.

As the result of numerical investigation with VR-KHNP, the following observations are made:

- The significant effects of groundwater flow direction is observed in the release rate at NFI for nuclides with high sorption coefficients in the aquifer (Ni, Nb, Sr, and Cs), while the effects are not significant for nuclides with low sorption coefficients (H, C, and I).

- Similarly, the analysis with the detailed waste vault geometry shows that the heterogeneity of radionuclide source affects significantly on release rate at NFI for high-sorption nuclides (Ni, Nb, Sr, and Cs). Little effect has been observed for low-sorption nuclides (H, C, and I).

- Only ^{3}H, ^{14}C, ^{59}Ni, ^{94}Nb, ^{129}I, and ^{238}U decay chain members are released through GBI by a significant rate. Other radionuclides attenuates significantly during the migration through aquifer compartments.

- As observed in Figure 5.5, the aquifer region at far field works as the natural barrier very efficiently, and reduces the peak release rate significantly for ^{63}Ni, ^{90}Sr, ^{99}Tc, ^{137}Cs, and ^{238}Pu decay chain members. However, it does not have so much effect on reduction of peak release rate for ^{3}H, ^{14}C, ^{129}I, ^{238}U decay chain members, and ^{238}Pu decay chain members.

- Change in the infiltration rate in the early times has a significant effects on the peak release rates of short-lived radionuclides at NFI. However, most of the short-lived radionuclides are not of concern at GBI since they decay out during the transport except for ^{3}H. Peak release rates of the high-sorption, long-lived radionuclides are not affected by the infiltration rate change in the early time.

- The environmental impact of the LLW repository is dominated by ^{129}I at the early times, and by ^{238}U and its daughters after 10^{6} yr. The peak environmental impact as about 10^{8} m^{3} and is due to ^{238}U decay chain members. Because of the long half-life of ^{238}U, almost all of the initial inventory of ^{238}U is eventually released into the environment. Therefore, in order to reduce the peak environmental impact, we need to reduce the initial inventory of ^{238}U.

A Running the Code

The code VR-KHNP is currently written in GNU Octave language. To run the code, GNU Octave is required. GNU Octave is available from `http://www.octave.org`. The current version of VR-KHNP is tested on GNU Octave v. 2.1.46.

To invoke the code, open a terminal, change to the directory that contains an input file, and type the following command:

```
octave vr-khnp.m input.txt
```

"`input.txt`" in the above line is the name of an input file. It should be replaced with the name of an existing input file in the directory.

As the code successfully runs, files named "`C-14.flux`," "`C-14.mass`" and so on are created. They are ASCII text files which contain the tabulated data of radionuclide flux and mass distributions for the decay chain whose first member is denoted in the file name.

B Format of Input Files

One or more ASCII text files are used as input to VR-KHNP code. An input file contains several *blocks* of data. A block starts with a `begin` statement, and ends with an `end` statement. All lines between these two statements are the contents of the block. Each block is assigned a unique name which is specified immediately after the keywords `begin` and `end` statements. There are blocks with fixed names that are always required in the input files (e.g., `GLOBAL`, `DECAY_CONSTANT`, and `DECAY_CHAIN` blocks are required). The names of other blocks are assigned by a user. Description on the contents of certain blocks is given in the following sections. The order of appearance of blocks is insignificant.

Comments can be inserted to the text, starting with a '#' character. All characters after the '#' in the line are regarded as comments and are ignored by the code. Comments can be inserted in any part of the input file.

White space characters (blank, tab, etc.), except end-of-line characters, are used only to divide a line into tokens. The number of spaces between two consecutive tokens is insignificant, i.e., any number of spaces can be put between two tokens. Lines that contains only white spaces and/or comments are insignificant, and are ignored. Therefore, empty lines and comment lines can be inserted in any part of the input file.

Input data can be spread over multiple files. For example, the user can store the `GLOBAL` block in a file called `specific_configuration.txt` and the rest of the blocks in a file called `common_data.txt`. In such cases, the command line to invoke the calculation should contain all file names:

```
octave vr-khnp.m specific_configuration.txt common_data.txt
```

A block, however, should be complete in one file, i.e., the `begin` statement and the `end` statement for a block must be in the same file.

Input files can contain blocks that are not used in the calculation. If an input file contains a block that is never refered to, the block is simply ignored by the program.

These flexible features make it possible to store data commonly used in many calculations in a single file and data specific to each calculation in separate files.

B.1 GLOBAL Block

A block named `GLOBAL` is required in input files for any calculation. Contents of this block describes the overview of the calculation, mostly by specifying what other blocks to use for detailed information.

Each line in `GLOBAL` block is actually a statement written in Octave language. This introduces convenience and flexibility in description of the problem while, on the other hand, requiring a user to understand

the basic syntax of Octave language. Although Octave syntax allows a statement to span over multiple lines, statement in `GLOBAL` block must be complete in a single line because the content of a block is processed line by line in the appearing order.

At the end of evaluation of contents of `GLOBAL` block, a structure variable `data` must contain the following fields:

`data.time` A list of block names for time points at which flux values are evaluated and written into the output files. (See Section B.9.) Each block corresponds to a separate time domain during which the physical properties are constant.

`data.sz.property` A list of block names for properties in saturated zone. (See Section B.4.) Each block corresponds to a separate time domain.

`data.sz.kd` A list of block names for distribution coefficients in saturated zone. (See Section B.7.) Each block corresponds to a separate time domain.

`data.initial_time` A column vector of times at which initial conditions are applied in the corresponding time domain. The times are usually the beginning of the corresponding time domain. For the first time domain, nuclide masses given in the initial inventory blocks are applied at the time denoted by the first element of vector `data.initial_time`. For the second time domain and later, the mass distribution at the time specified in this vector is evaluated based on the conditions in the previous time domain and is used as the initial condition for the current time domain.

`data.input_in_activity` This field should be set to 0 if the values in the initial inventory blocks (Section B.6) are given in terms of number of atoms ([atoms], [mol], etc.), 1 if they are given in terms of activity ([Bq], [Ci], etc.). This distinction is necesarry for decay chain with multiple member nuclides.

`data.output_in_activity` If the flux and the mass in output files are to be given in terms of number of atoms, this field should be set to 0. If they are to be given in terms of activity, this field should be set to 1. If `input_in_activity` and `output_in_activity` are both 1, or both 0, then the unit of mass in output is the same as that of initial inventory in the input files, and the unit of flux in output is [$*$/yr] where [$*$] is the unit of the initial inventory.

`data.uz` This field is a list of structures for unsaturated zone columns. In the example below, `uz1` is a structure for one unsaturated zone column. Each field of `uz1` is assigned a value first, and `uz1` is used to form the list `data.uz`. In this example, the list `data.uz` consists of only a single element `uz1` (i.e., there is only a singe column of unsaturated zone in the calculation). If there are more than one column of unsaturated zone, more structures (e.g., `uz2`, `uz3`, ...) should be defined and listed as elements in the list `data.uz`. `uz1` is a temporary variable only to construct the list `data.uz`.

Therefore it could have been called something else. The unsaturated zone structure consists of the following fields:

property A list of block names for properties in unsaturated zone. (See Section B.5.) Each block corresponds to a separate time domain.

kd A list of block names for distribution coefficients in unsaturated zone. (See Section B.8.) Each block corresponds to a separate time domain.

inventory Name of the initial inventory block for this unsaturated zone.

position The horizontal distance of the closest boundary of the unsaturated zone column from the end point of aquifer (GBI).

length The horizontal length of the unsaturated zone column. The length is measured horizontally along the flow direction in the saturated zone.

```
begin GLOBAL
   data.time = list( "time1", "time2", "time3" );
   data.sz.property = list( "aquifer", "aquifer", "aquifer" );
   data.sz.kd = list( "Kd_aquifer", "Kd_aquifer", "Kd_aquifer" );
   data.sz.dispersivity = 20.0;  ## [m] longitudinal dispersivity
   data.initial_time = [ 0; 100; 500 ];  ## [yr]
   data.input_in_activity = 1;  ## 1 if inventory is given in Bq or Ci
   data.output_in_activity = 1;  ## 1 if output is given in Bq or Ci

   uz1.property = list( "v21", "v22", "v23" );
   uz1.kd = list( "Kd_vault", "Kd_vault", "Kd_vault" );
   uz1.inventory = "ii-total";
   uz1.position = 210;  ## [m] distance from the measurement point
   uz1.length = 50;  ## [m] in the direction of flow in aquifer

   data.uz = list( uz1 );
end GLOBAL
```

B.2 DECAY_CONSTANT Block

Decay constants for all the nuclides are to be listed in this block. Each line in this block must contain the name of a nuclide and its decay constant [1/yr] in this order. A nuclide name can be any sequence of non-blank characters, and it is not required to have a certain format (i.e., it can be `U-235`, `235U`, and even `imaginary_nuclide_A`). However, each nuclide must be given a unique name. All nuclide names that appear in the other part of the input files must be declared in this block with their decay constants. Order of appearance of nuclide names is not significant in the calculation.

```
begin DECAY_CONSTANT
   #nuclide decay_constant[1/yr]
   H-3     5.59e-02
```

```
   C-14    1.21e-04
   Co-60   1.32e-01
   # ...
end DECAY_CONSTANT
```

B.3 DECAY_CHAIN Block

A block with the name `DECAY_CHAIN` must be provided in the input files. Each line in this block specifies a radioactive decay chain and its member nuclides. Each line must contain one or more nuclide names defined in `DECAY_CONSTANT` block. Calculation is performed for each decay chain separately in the appearing order.

```
begin DECAY_CHAIN
   ## single-member decay chains
   H-3
   C-14
   Co-60

   ## multi-member decay chain
   U-238 U-234 Th-230 Ra-226 Pb-210 Po-210
end DECAY_CHAIN
```

B.4 Blocks for Properties of Saturated Zone

This block specifies the nuclide-independent properties of the compartments in the saturated zone for a certain time span. Its block name must be specified in `data.sz.property` variable in `GLOBAL` block. Porosity, saturation, bulk density [kg/m^3], and Darcy velocity [m/yr] of groundwater in the saturated zone are listed in a single line in this order.

```
begin aquifer
   0.25 1.0 2500 10.0
end aquifer
```

B.5 Blocks for Properties of Unsaturated Zone

Each line in this block specifies the nuclide-independent properties of a compartment in the unsaturated zone for a certain time period. The first line contains the properties in the topmost compartment, the second line the second to the topmost, and so on. The last line thus corresponds to the bottom compartment in the unsaturated zone immediately above the saturated zone. The number of compartments is determined by the number of lines in this block. Each line contains the dimension of the compartment in the flow direction [m], porosity, saturation, bulk density [kg/m^3], and Darcy velocity of groundwater [m/yr] in the compartment in this order.

```
begin v11  ## vault type1 time1 (0-100 yr)
   8.2 0.30 0.5 2000 3.5e-4 ## waste type1
   0.5 0.12 0.5 2500 3.5e-4 ## concrete
   3.0 0.30 0.7 1800 3.5e-4 ## soil
end v11
```

Different columns of unsaturated zone can have different number of compartments. However, the number of compartments in any column may not change with time.

B.6 Blocks for Initial Inventory

Blocks for initial inventory in the unsaturated zone column must provide the inventory for each nuclide and for each compartment in the column. Each line in this block describes for a nuclide. A line must contain the nuclide name (that must be defined in `DECAY_CONSTANT` block), its initial inventory in the top compartment of the UZ column, and then the inventory in the second compartment, and so on. Thus, each line must contain the same number of inventory values as the number of compartments in the UZ column. Depending on the units of the inventory given in this block, the parameter `data.input_in_activity` must be adjusted to a proper value.

```
begin ii1  ## vault type1
   #nuclide inventory_in_waste in_concrete in_soil
   H-3    2.97e+11 0 0
   C-14   2.67e+11 0 0
   Co-60  1.82e+13 0 0
   # ...
end ii1
```

B.7 Blocks for Distribution Coefficients in Saturated Zone

This block specifies the distribution coefficient values in saturated zone, $K_{\mathrm{d}_{\mathrm{SZ}}}^{(i)}$, for all nuclides. Each line consists of two fields: the nuclide name and the distribution coefficient value $[\mathrm{m}^3/\mathrm{kg}]$.

```
begin Kd_aquifer
   #nuclide Kd[m3/kg]
   H-3           0
   C-14   1.00e-02
   Co-60  1.00e+00
   # ...
end Kd_aquifer
```

B.8 Blocks for Distribution Coefficients in Unsaturated Zone

This block specifies the distribution coefficient values in unsaturated zone, $K_{\mathrm{d}l,m}^{(i)}$, for all nuclides. Each line starts with the nuclide name followed by the distribution coefficient values [m^3/kg]. Each line must contain the same number of Kd values as the number of compartments in the UZ column.

```
begin Kd_vault
   H-3           0        0        0
   C-14   2.50e+00 2.50e+00 5.00e-03
   Co-60  2.00e-02 2.00e-02 1.50e-02
   # ...
end Kd_vault
```

B.9 Blocks for Time Points

This block specifies the time points (within the corresponding time domain) at which the masses and fluxes are evaluated and printed into output files.

As is the case with `GLOBAL` block, each line in this block is a statement written in octave language. At the end of evaluation of this block, the variable `data.time` must contain a row vector of time points [yr].

One of the simplest example is as follows:

```
begin time1
   data.time = [ 0, 10, 20, 30, 40, 50, 60, 70, 80, 90, 100 ];
end time1
```

This specifies to evaluate at 0 yr, 10 yr, 20 yr, . . . , and at 100 yr.

If a user wants to evaluate further, the following block can be used:

```
begin time1
   data.time = [ 0, 10, 20, 30, 40, 50, 60, 70, 80, 90, 100 ];
   data.time = [ data.time, 120, 140, 160, 180, 200 ];
end time1
```

The above block can actually be simplified, using a convenient syntax of Octave. The example below creates the same vector `data.time` as the previous example.

```
begin time1
   data.time = [ (0:10:100), (120:20:200) ];
end time1
```

C Input File for the Benchmark Test Calculation

```
begin GLOBAL
   data.time = list( "time1", "time2", "time3" );
   data.sz.property = list( "aquifer", "aquifer", "aquifer" );
   data.sz.kd = list( "Kd_aquifer", "Kd_aquifer", "Kd_aquifer" );
   data.sz.dispersivity = 20.0;  ## [m] longitudinal dispersivity
   data.initial_time = [ 0; 100; 500 ];  ## [yr]
   data.input_in_activity = 1;  ## 1 if inventory is given in Bq or Ci
   data.output_in_activity = 1;  ## 1 if output is given in Bq or Ci

   uz1.property = list( "v21", "v22", "v23" );
   uz1.kd = list( "Kd_vault", "Kd_vault", "Kd_vault" );
   uz1.inventory = "ii-total";
   uz1.position = 180;  ## [m] distance from the measurement point
   uz1.length = 10;  ## [m] in the direction of flow in aquifer

   data.uz = list( uz1 );
end GLOBAL

begin DECAY_CHAIN
   H-3
   C-14
   Co-60
   Ni-59
   Ni-63
   Sr-90
   Nb-94
   Tc-99
   I-129
   Cs-137
   U-238 U-234 Th-230 Ra-226 Pb-210 Po-210
   Pu-238 U-234 Th-230 Ra-226 Pb-210 Po-210
   Pu-239 U-235 Pa-231 Ac-227
end DECAY_CHAIN

begin aquifer
   ## columns
   ## 1 : porosity [-]
   ## 2 : saturation [-]
   ## 3 : bulk density [kg/m3]
   ## 4 : darcy velocity of water [m/yr]

   0.25 1.0 3333 10.0
end aquifer

## vault properties
## columns
## 1 : dimension in the flow direction [m]
## 2 : porosity [-]
## 3 : saturation [-]
```

```
## 4 : bulk density [kg/m3]
## 5 : darcy velocity of water [m/yr]

begin v21  ## vault type2&3 time1
   8.2 0.12 0.5 2840 3.5e-4 ## waste type2 & 3
   0.5 0.12 0.5 2840 3.5e-4 ## concrete
   1.0 0.30 0.7 2571 3.5e-4 ## soil
   1.0 0.30 0.7 2571 3.5e-4 ## soil
   1.0 0.30 0.7 2571 3.5e-4 ## soil
end v21

begin v22  ## vault type2&3 time2
   8.2 0.12 0.5 2840 3.5e-2 ## waste type2 & 3
   0.5 0.12 0.5 2840 3.5e-2 ## concrete
   1.0 0.30 0.7 2571 3.5e-2 ## soil
   1.0 0.30 0.7 2571 3.5e-2 ## soil
   1.0 0.30 0.7 2571 3.5e-2 ## soil
end v22

begin v23  ## vault type2&3 time3
   8.2 0.12 0.5 2840 3.5e-1 ## waste type2 & 3
   0.5 0.12 0.5 2840 3.5e-1 ## concrete
   1.0 0.30 0.7 2571 3.5e-1 ## soil
   1.0 0.30 0.7 2571 3.5e-1 ## soil
   1.0 0.30 0.7 2571 3.5e-1 ## soil
end v23

begin DECAY_CONSTANT
#  nuclide decay_constant[1/yr]
   H-3     5.59e-02
   C-14    1.21e-04
   Co-60   1.32e-01
   Ni-59   9.19e-06
   Ni-63   7.22e-03
   Sr-90   2.38e-02
   Nb-94   3.41e-05
   Tc-99   3.25e-06
   I-129   4.41e-08
   Cs-137  2.31e-02
   Pb-210  3.11e-02
   Po-210  1.83e-00
   Ra-226  4.33e-04
   Ac-227  3.18e-02
   Th-230  9.00e-06
   Pa-231  2.11e-05
   U-234   2.83e-06
   U-235   9.85e-10
   U-238   1.55e-10
   Pu-238  7.90e-03
   Pu-239  2.88e-05
end DECAY_CONSTANT

## initial inventory
```

```
## columns
## 1 : nuclide name
## 2 : in waste
## 3 : in concrete
## 4 : in soil

begin ii-total
   H-3    2.67e+13 0 0 0 0
   C-14   1.68e+13 0 0 0 0
   Co-60  1.73e+14 0 0 0 0
   Ni-59  3.64e+12 0 0 0 0
   Ni-63  9.51e+13 0 0 0 0
   Sr-90  1.39e+12 0 0 0 0
   Nb-94  1.00e+11 0 0 0 0
   Tc-99  4.07e+10 0 0 0 0
   I-129  1.25e+10 0 0 0 0
   Cs-137 6.09e+13 0 0 0 0
   Pb-210         0 0 0 0 0
   Po-210         0 0 0 0 0
   Ra-226         0 0 0 0 0
   Ac-227         0 0 0 0 0
   Th-230         0 0 0 0 0
   Pa-231         0 0 0 0 0
   U-234          0 0 0 0 0
   U-235  1.91e+08 0 0 0 0
   U-238  4.75e+10 0 0 0 0
   Pu-238 1.28e+11 0 0 0 0
   Pu-239 5.89e+10 0 0 0 0
end ii-total

## distribution coefficient in aquifer [m3/kg]
## columns
## 1 : nuclide name
## 2 : Kd in aquifer [m3/kg]
begin Kd_aquifer
   H-3           0
   C-14   1.00e-02
   Co-60  1.00e+00
   Ni-59  1.00e+00
   Ni-63  1.00e+00
   Sr-90  2.00e-02
   Nb-94  1.00e+00
   Tc-99  1.00e+02
   I-129  5.00e-03
   Cs-137 1.00e-01
   Pb-210 1.00e+02
   Po-210 1.00e+02
   Ra-226 1.00e+02
   Ac-227 1.00e+02
   Th-230 1.00e+02
   Pa-231 1.00e+02
   U-234  1.00e+02
   U-235  1.00e+02
```

```
   U-238  1.00e+02
   Pu-238 5.00e+00
   Pu-239 5.00e+00
end Kd_aquifer

## distribution coefficient in vault [m3/kg]
## columns
## 1 : nuclide name
## 2 : in waste [m3/kg]
## 3 : in concrete [m3/kg]
## 4 : in soil [m3/kg]

begin Kd_vault
   H-3           0        0        0        0        0
   C-14   2.50e+00 2.50e+00 5.00e-03 5.00e-03 5.00e-03
   Co-60  2.00e-02 2.00e-02 1.50e-02 1.50e-02 1.50e-02
   Ni-59  2.00e-02 2.00e-02 4.00e-01 4.00e-01 4.00e-01
   Ni-63  2.00e-02 2.00e-02 4.00e-01 4.00e-01 4.00e-01
   Sr-90  2.50e-03 2.50e-03 1.50e-02 1.50e-02 1.50e-02
   Nb-94  5.00e-01 5.00e-01        0        0        0
   Tc-99  5.00e-01 6.00e-01 1.00e-04 1.00e-04 1.00e-04
   I-129  6.00e-04 6.00e-04 1.00e-03 1.00e-03 1.00e-03
   Cs-137 2.50e-04 2.50e-04 3.00e-01 3.00e-01 3.00e-01
   Pb-210 2.00e+00 2.00e+00        0        0        0
   Po-210 2.00e+00 2.00e+00        0        0        0
   Ra-226 2.00e+00 2.00e+00        0        0        0
   Ac-227 2.00e+00 2.00e+00        0        0        0
   Th-230 2.00e+00 2.00e+00        0        0        0
   Pa-231 2.00e+00 2.00e+00        0        0        0
   U-234  2.00e+00 2.00e+00        0        0        0
   U-235  2.00e+00 2.00e+00        0        0        0
   U-238  2.00e+00 2.00e+00        0        0        0
   Pu-238 4.00e+00 4.00e+01        0        0        0
   Pu-239 4.00e+00 4.00e+01        0        0        0
end Kd_vault

begin time1
   data.time = [ (0:1:10), (12:2:20), (25:5:50), (60:10:100) ];
end time1

begin time2
   data.time = [ (100:20:200), (250:50:500) ];
end time2

begin time3
   data.time = [ (500:100:1000) ];
   data.time = [ data.time, (1.2e+3:0.2e+3:2.0e+3) ];
   data.time = [ data.time, (2.5e+3:0.5e+3:5.0e+3) ];
   data.time = [ data.time, (6.0e+3:1.0e+3:10.0e+3) ];
   data.time = [ data.time, (1.2e+4:0.2e+4:2.0e+4) ];
   data.time = [ data.time, (2.5e+4:0.5e+4:5.0e+4) ];
   data.time = [ data.time, (6.0e+4:1.0e+4:10.0e+4) ];
   data.time = [ data.time, (1.2e+5:0.2e+5:2.0e+5) ];
```

```
   data.time = [ data.time, (2.5e+5:0.5e+5:5.0e+5) ];
   data.time = [ data.time, (6.0e+5:1.0e+5:10.0e+5) ];
end time3
```

References

[1] J. AHN, D. KAWASAKI, and P. L. CHAMBRÉ, "Relationship among Performance of Geologic Repositories, Canister-Array Configuration, and Radionuclide Mass in Waste," *Nucl. Technol.*, **140**, *1*, 94 (2002).

[2] D. Kawasaki, J. Ahn, P. L. Chambré, and W. G. Halsey, "Congruent Release of Long-Lived Radionuclides from Multiple Canister Arrays," *Nucl. Technol.*, in press.

[3] K. Tsujimoto and J. Ahn, "Development of Object-Oriented Simulation Code for Repository Performance Assessment," 1999 Winter Meeting, Long Beach, November 14–18, 1999, American Nuclear Society (1999).

[4] K. TSUJIMOTO, D. KAWASAKI, J. AHN, and P. L. CHAMBRÉ, "Virtual Repository (VR) Version 1.0 Operation Manual," Department of Nuclear Engineering, University of California, Berkeley (2000).

[5] J. W. Park, S. M. Park, C. L. Kim, and C. W. Chung, "Development and Implementation of a Perfomance Assessment Approach to Determine Waste Concentration Limits for a Near-Surface Radioactive Waste Disposal Facility in Korea," SPECTRUM 2002.

[6] J. W. Park, C. L. Kim, K. M. Chang, and M. J. Song, "Scenario Development Methodology for Perfomance Assessment of Near-Surface LILW Repository Based on FEPS and Interaction Matrix Approach," Waste Management 2002, February 24–28, 2002, Tucson, Arizona.

[7] W. Zhou, M. W. Kozak, J. W. Park, C. L. Kim, and C. H. Kang, "Development of SAGE, A Computer Code for Safety Assessment Analyses for Korean Low-Level Radioactive Waste Disposal," KAIF-KNS Conference, 2002.

[8] J. AHN, "An Environmental Impact Measure for Nuclear Fuel Cycle Evaluation," *Journal of Nuclear Science and Technology*, in press.

[9] Code of Federal Regulation, Title 10, Part 20, "Standards for Protection against Radiation," US NRC.

[10] J. AHN, D. KAWASAKI, P. L. CHAMBRÉ, “Environmental Impact and Capacity Expansion of Geologic Repository,” Global 2003, New Orleans, Louisiana, American Nuclear Society, (2003).